CDF/ANAL/ELECTROWEAK/CDFR/10115
Version 2.10
September 6, 2010

Study of the Di-jet mass spectrum of jets produced in association with a W boson in 4.3 fb^{-1}

Alberto Annovi[1]
INFN Frascati, Italy

Pierluigi Catastini[2]
Fermilab

Viviana Cavaliere[3]
University of Siena, INFN Pisa, Italy and Fermilab

Luciano Ristori[4]
INFN Pisa, Italy and Fermilab

Abstract

We describe a study of the di-jet mass of jets produced in association with $W \rightarrow l\nu$. A data sample of high p_T electrons and muons corresponding to approximately 4.3 fb^{-1} of integrated luminosity is used to reconstruct W boson in its leptonic decay . We then look for a di-jet candidate in the event by selecting exactly two additional jets passing selections. A fit to the invariant mass distribution M_{jj} of the two jets is performed. An excess of of events over expectation for known processes is observed in the mass region [120, 160] GeV/c^2. If we assume the presence of an additional gaussian component, we obtain a p-value of $7.4 * 10^{-4}$ corresponding to a significance of 3.2 σ when standard systematics sources are considered.

[1]alberto.annovi@lnf.infn.it
[2]catasti@fnal.gov
[3]viviana@fnal.gov
[4]luciano@fnal.gov

Contents

1 Introduction

In [1] we observed WW/WZ production in the $l\nu jj$ final state with a statistical significance of 5.2 σ by looking for a bump in the di-jet mass spectrum. At the time, a small excess in the di-jet mass spectrum with respect to the estimated background was visible around 150 GeV/c^2. A unique feature of bump searches in the invariant mass spectrum is that very few assumptions (if any) are needed on the physical process: signature due to completely unexpected phenomena manifest themselves as a resonance/peak in the invariant mass distribution.
In the process of improving WW/WZ production cross section measurement we slightly modified our selections. The excess already visible in [1] was still in place and we decided to perform a search for an additional resonance in the di-jet distribution and estimate the corresponding significance.
In this note, after showing and motivating the changes we made to the original WW/WZ analysis, we describe a search for an unexpected resonance in the di-jet mass spectrum using 4.3 fb^{-1} collected by the CDF detector.

The main changes with respect to original $WW/WZ \to l\nu jj$ analysis are:

1. We use Level 5 jet corrections, instead of Level 7.

2. We require *exactly* two jets in the event that satisfies selection criteria. This is in contrast to the previous requirement of *at least* two jets. With this choice we expect to select events with a clean topology and less prone to pathology due to multiple jets.

3. Since we look for high mass resonances, we require the two jets to have $E_T > 30$ instead of $E_T > 20$. In the WW/WZ search we wanted to keep the jet threshold as low as possible to avoid sculpting of the di-jet spectrum near the W/Z mass region. Jets with higher E_T are expected to be better defined and reconstructed.

4. We set up a combined fit for the muon and electron samples.

The details about the electron selection, the muon selection and the measurement of the W inclusive cross section are discussed in [2], and will not be further discussed in this note.

2 Data Sample

We use the high P_T electron and muon datasets up to period 23 for a total luminosity of 4.3 fb^{-1}.
For the electron decay channel we use the datasets bhelkd, bhelkh, bhelki, bhelmi, bhelmj, bhelmk and bhelmm selected using the ELECTRON_TRIGGER_18 trigger. For muon channel we use the datasets bhmukd, bhmukh, bhmuki, bhmumi, bhmumj, bhmumk and bhmumm. The events in these datasets are triggered by:

- CMUP: run $\leq$ 229763: MUON_CMUP_18_V || MUON_CMUP_18_L2_PT15V
- 229763 $<$ run: MUON_CMUP18_V
- CMX: run $\leq$ 200272: MUON_CMX18_V || MUON_CMX18_L2_PT15_V
- 200272 $<$ run $\leq$ 226194: MUON_CMX18_L2_PT15_V || MUON_CMX18_L2_PT15_LUMI_200_V
- 226194 $<$ run $\leq$ 257201: MUON_CMX18_&_JET10_V || MUON_CMX18_&_JET10_LUMI_270_V || MUON_CMX18_&_JET10_DPS_V
- 257201 $<$ run: MUON_CMX18_V

Events have been reconstructed using version 6.1.4 of the offline software for data up to period 17 and version 6.1.6 for later data. We require the silicon to be fully operational using the Silicon Good Run List version 33 with logic (1,1,0,1) for electrons and (0,1,4,1) for muons.

3 Monte Carlo Samples

The Monte Carlo samples are generated with Alpgen v2.10 prime and PYTHIA v. 6.325 for showering. Each sample is weighted to the same equivalent integrated luminosity according to:

$$weight = \frac{\int \mathcal{L} dt_{wanted} * \sigma_{ALPGEN}}{number\ of\ events}. \quad (1)$$

In Table 1 - 4 there is a list of all the MC samples used for the analysis. In the first column is reported the MC sample that was generated to match the luminosity profile of data from period 0-8 and in the second column the corresponding high luminosity sample. Simply adding the two we get the luminosity profile of data up to period 17. The weight of the sum is given by:

$$weight = \frac{\int \mathcal{L} dt_{wanted} * \sigma_{ALPGEN}}{N_{gen,lowlumi} + N_{gen,highlumi}}. \quad (2)$$

Furthermore in order to mimic the same luminosity spectrum of data after p17, MC is reweighted to match the number of the vertices in the event seen in data (see Fig 1 and Fig 2). The reweight for the number of vertices has a negligible effect on the dijet mass spectra, but becomes relevant when we compare quantities strongly affected by the event activity such as the angle between the $\not\!\!E_T$ and the low energy closest jet or the angle between the calorimetric $\not\!\!E_T$ and the $\not\!\!P_T$.

sample low lumi	sample high lumi
Diboson	
ihhp1a	ihhp1a
jhhp1a	jhhp1a
khhp1a	khhp1a
W ($e\nu$)+jets	
ptopw0	utop00
ptopw1	utop01
ptop2w	utop02
ptop3w	utop03
ptop4w	utop04
W ($\mu\nu$)+jets	
ptopw5	utop05
ptopw6	utop06
ptop7w	utop07
ptop8w	utop08
ptop9w	utop09
W ($\tau\nu$)+jets	
utopw0	utop10
utopw1	utop11
utop2w	utop12
utop3w	utop13
utop4w	utop14
top	
ttop25	ttop25
single top	
stop26	stop26
stop27	stop27

Table 1: List of the Monte Carlo samples.

low lumi sample	high lumi
Z(e^+e^-)+jets	
ztopp0	btopz0
ztopp1	btopz1
ztop2p	btopz2
ztop3p	btopz3
ztop4p	btopz4
Z($\mu^+\mu^-$)+jets	
ztopp5	btopz5
ztopp6	btopz6
ztop7p	btopz7
ztop8p	btopz8
ztop9p	btopz9
Z($\tau^+\tau^-$)+jets	
ztopt3	btopza
ztopt2	btopzb
ztopt4	btopzc
xtopt2	
xtopt3	
xtopt4	

Table 2: List of the Monte Carlo samples.

low lumi sample	high lumi
DY	
xtop0p	
xtop1p	
xtop2p	
xtop3p	
xtop4p	
xtop5p	
xtop6p	
xtop7p	
xtop8p	
xtop9p	

Table 3: List of the Monte Carlo samples.

low lumi Sample	high lumi Sample
DY	
ytop0p	
ytop1p	
ytop2p	
ytop3p	
ytop4p	
ytop5p	
ytop6p	
ytop7p	
ytop8p	
ytop9p	

Table 4: List of the Monte Carlo samples.

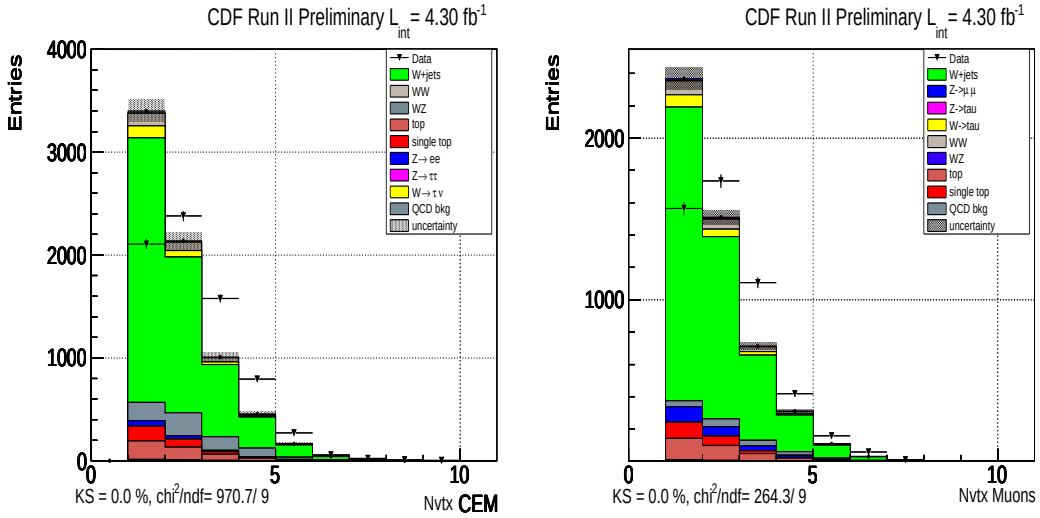

Figure 1: nvtx distribution for electrons and muons before reweight.

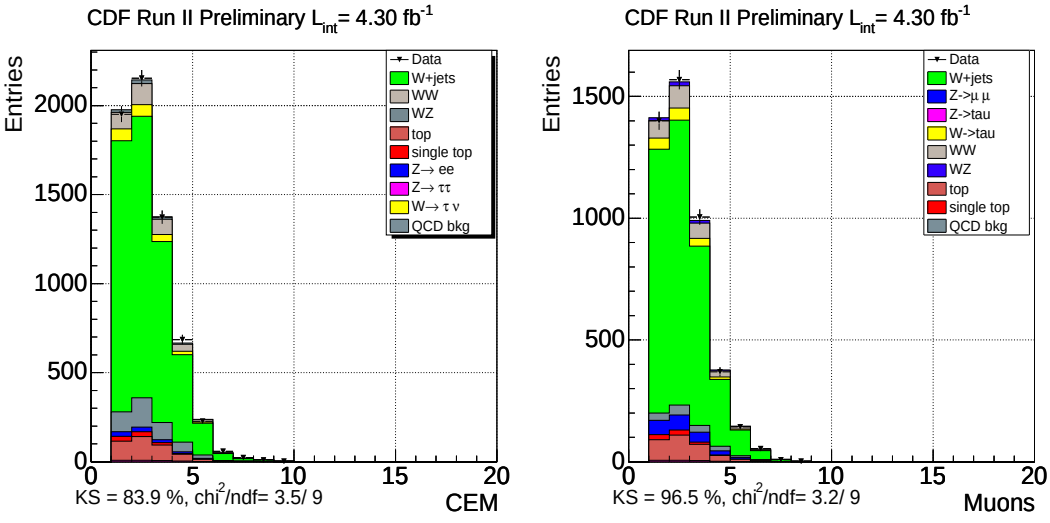

Figure 2: nvtx distribution for electrons and muons after reweight.

4 Missing transverse energy

$\not\!\!E_T$ is calculated with a vector sum over the tranverse energies of the calorimeter towers. $\not\!\!E_T$ is corrected for the position of the primary vertex of the event, which, if not at the center of the detector, will cause an adjustment in the direction of the vector associated with each tower. Since muon carries substantial energy but deposits very little in the calorimeter, in events containing a muon, the transverse energy of the muon is included in the calculation. Moreover, since a muon is also matched to a calorimeter cluster with minimum-ionizing energy, the energy of its associated cluster must be subtracted from its total energy, otherwise the calorimeter energy would be counted twice. Furthermore, when jet corrections are applied to jets, the missing transverse energy is corrected as well.

5 Jets

Jets are reconstructed using JETCLU algorithm with cone size 0.4. If an electron or a muon is found in cone $\Delta R = 0.52$ around the jet, the jet is removed. We apply L5 correction (absolute corrections) that correct for the calorimeter energy scale, the η dependence, multiple interactions, and for calorimeter non-linearity.

6 Event vetoes

We apply a cosmic veto and Z veto to the events. The cosmic veto is the standard top-ntuple procedure. The Z boson veto looks for a very loosely identified lepton (including a high-momentum track with no other tracks nearby) with the opposite charge of the identified tight lepton. If the invariant mass of the two falls near the Z boson mass (66−116 GeV), the event is rejected. This leaves very little residual contamination from Z + jets events.

7 $W \rightarrow e\nu$ selection

$W \rightarrow e\nu$ events are selected looking for one tight electron fulfilling the requirements of Tab. 5 and requiring $\not\!\!E_T > 25\ GeV$. $\not\!\!E_T$ is corrected for loose muons in the event and for jets with $E_{Traw} > 8\ GeV$.

The W is reconstructed requiring the transverse mass ($M_T(W)$) to be $> 30\ GeV/c^2$. This cut significantly reduces the QCD background and has small impact on real W.

Variable	Cut
Region	central
Track	yes
Iso/E_T	≤ 0.1
E_T	> 20 GeV
P_T	> 10 GeV
Track $\lvert Z_0 \rvert$	≤ 60cm
E/P	≤ 2 (unless $p_t \geq 50$ GeV/c)
Had/Em	$\leq 0.055 + 0.00043 \cdot E$
Signed CES ΔX	$-3.0 \leq q\Delta X \leq 1.5$
CES ΔX	< 3cm
Lshr	< 0.2
CES Strip χ^2	$\leq$10
Fiducial	yes

Table 5: Electron selections.

Variable	Cut
Iso/P_T	≤ 0.1
P_T	> 20 GeV
Track $\lvert Z_0 \rvert$	≤ 60cm
CMU Fid	$x - fid < 0$cm, $z - fid < 0$cm
CMP FId	$x - fid < 0$cm, $z - fid < -3$cm
CMX Fid	$x - fid < 0$cm, $z - fid < -3$cm
E_{em}	$\leq 2 + max(0, (p - 100) \cdot 0.0115)$
E_{had}	$\leq 6 + max(0, (p - 100) \cdot 0.028)$
COT Ax hits / Ax Seg	$\geq 5/\geq 3$
COT Ax hits / Ax Seg	$\geq 5/\geq 3$
COT χ^2	< 2.3
Track no si hits $\lvert d_0 \rvert$	< 0.2cm
Track si hits $\lvert d_0 \rvert$	< 0.02cm
ρ_{exit}	$> 140cm$ if CMX
$\lvert \Delta X_{CMU} \rvert$	≤ 7cm
$\lvert \Delta X_{CMP} \rvert$	≤ 5cm
$\lvert \Delta X_{CMX} \rvert$	≤ 6cm
No muons in bluebeam	run <154449
No muons in keystone	run <186598
No muons in miniskirt	run <186598
Larry corrections	data only

Table 6: Muon selections.

8 $W \to \mu\nu$ selection

CMUP and CMX muons are reconstructed separately according to the selection of Table 6; also for muons, we require $\not\!\!E_T > 25\ GeV$ after correcting $\not\!\!E_T$ for loose muons and jet with $E_T > 8\ GeV$ (Level 5 correction). In addition, we require $M_T(W) > 30\ GeV/c^2$.

9 Sample Composition

We consider the following Standard Model processes:

- Diboson production: WW and WZ
- $W \to l\nu$ + n jets ; $n \geq 0$, $l = e, \mu, \tau$
- $Z \to ll$ + n jets ; $n \geq 0$, $l = e, \mu, \tau$
- $t\bar{t}$ + single top
- QCD

The only component that is not extracted by Monte Carlo is the QCD contribution. The other sources are estimated by the MC samples of Table 1 - 4.
QCD background is estimated using the technique described in [4] [5]. A fit to the $\not\!\!E_T$ distribution in the range [0,200] GeV is performed after removing the $\not\!\!E_T > 25$ GeV requirement. Fig.3 shows the QCD fits when our analysis selections (described in section 10 and without the $\not\!\!E_T$ cut) are applied. In the case of muons, the QCD template is extracted from the high isolation sample ($Iso > 0.2$), while in the case of the electron we use the antielectron sample. The antielectron sample is obtained by looking for electron candidates that pass the kinematic selections but fail at least two of the electron id requirements, as defined in [5]. For all the other components, the corresponding templates are extracted from Monte Carlo.

10 Dijet Candidate Selection

We want to keep the search analysis as close as possible to the original diboson analysis and we leave the selection as it was besides the increased jet E_T cut. In fact, in the standard diboson selection we required jets with $E_T > 20$ GeV. This was motivated by the need to keep the jet E_T threshold as low as possible in order not to sculpt the m_{jj} shape of the background under the dijet signal. However, in the high mass resonance search we are looking for an heavier object and we are allowed to increase the jet E_T threshold. Selecting more energetic jets has a clear advantages: jets with higher E_T are better defined and better described by MC. We choose to require jets

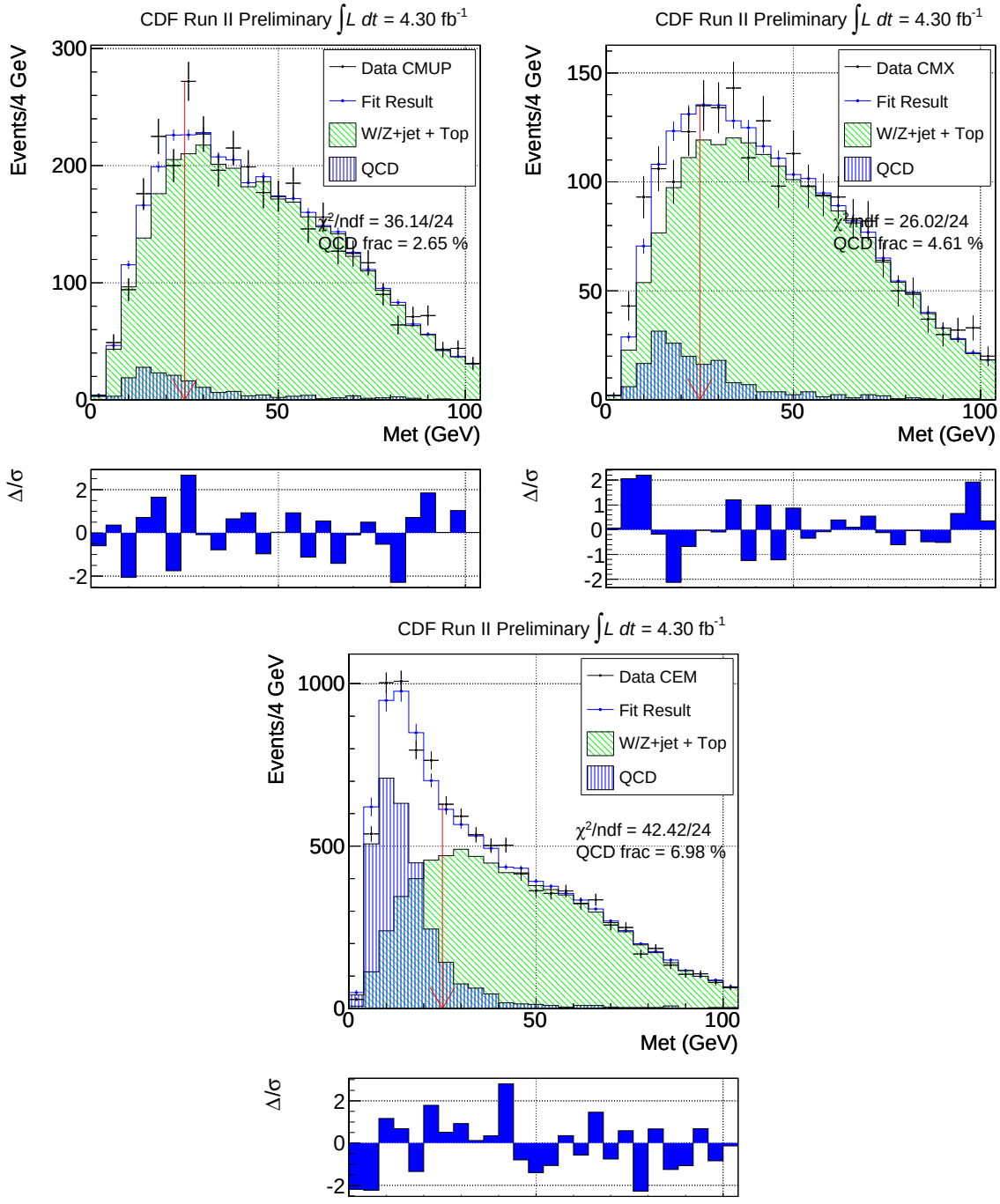

Figure 3: Upper left: $\not\!\!E_T$ fit of the QCD background for CMUP. Upper right: $\not\!\!E_T$ fit of the QCD background for CMX. Bottom: $\not\!\!E_T$ fit of the QCD background for CEM. These fits refere to the di-jet selection.

with $E_T > 30$ GeV. Another difference with respect to the diboson analysis is that now we require *exactly* two jets satisfying selection criteria. With this choice we expect to select events with a clean topology and less prone to pathology due to multiple jets. Jets are reconstructed using JETCLU04 and corrected at level 5; in addition they are required to have $|\eta| < 2.4$ and $\Delta\eta_{j1j2} < 2.5$. As already mentioned, we changed the jet energy corrections from level 7 to level 5 with respect to [1]. We also require $p_T(jj) > 40\ GeV/c$ for the di-jet candidate. The agreement between data and MC is not satisfactory for $p_T(jj) < 40\ GeV/c$ [1]. For this reason and similarly to the previous analysis [2], we decide to consider the $p_T > 40\ GeV/c$ subsample only since we believe that for $p_T < 40\ GeV/c$ more careful understanding is required. As in [1], we apply an additional cut $\Delta\phi_{met,jet1} > 0.4$ to reject part of the QCD background. This selection is applied also to sample used in the QCD fit of Section 9. In what follow, when we refer to muon sample we consider CMUP and CMX samples together and when we refer to the electron sample we consider CEM sample. In Tab. 7 we show the estimated number of events for our muon and electron selected samples while in Fig.4 we overimpose the M_{jj} spectra for data and background expectation: a clear mismodeling can be observed in the region around 140 GeV/c^2 both in muons and electrons.

Sample	**CEM**	**CMUP + CMX**
MC W +jets	4577 ± 137	3364 ± 100
MC Z+jets	96 ± 9	191 ± 19
diboson	405 ± 24	302 ± 18
top	412 ± 49	310 ± 37
QCD (from data)	384 ± 96	108 ± 27
QCD + MC	5874	4275
data	5917 ± 78	4197 ± 65

Table 7: Expected number of events of each contribution for $M_{jj} \in$ [28,200] GeV/c^2.

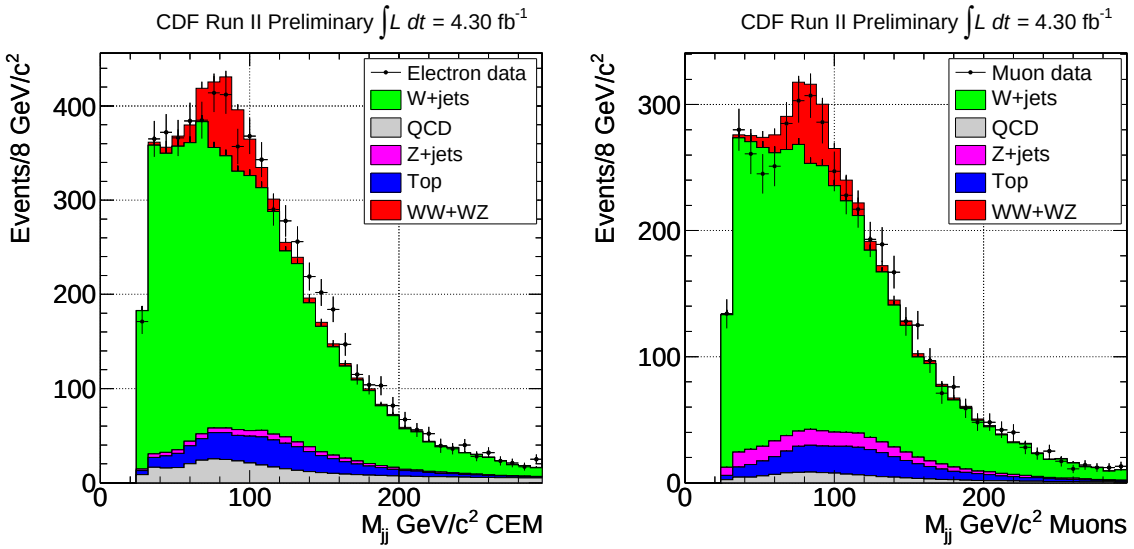

Figure 4: Expected M_{jj} distribution overimposed to data; left: electrons; right: muons.

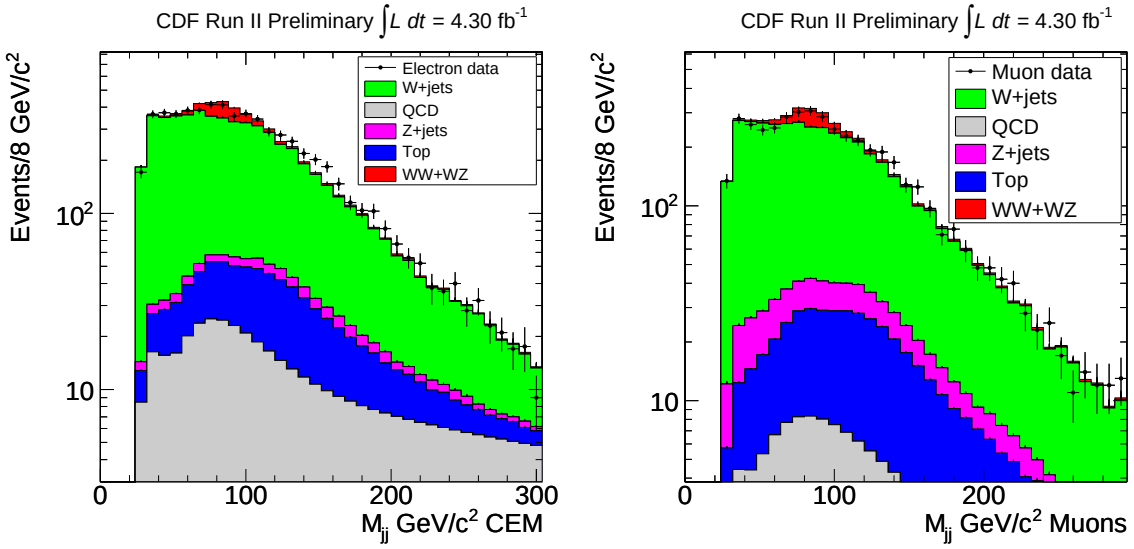

Figure 5: Expected M_{jj} distribution overimposed to data in log scale; left: electrons; right: muons.

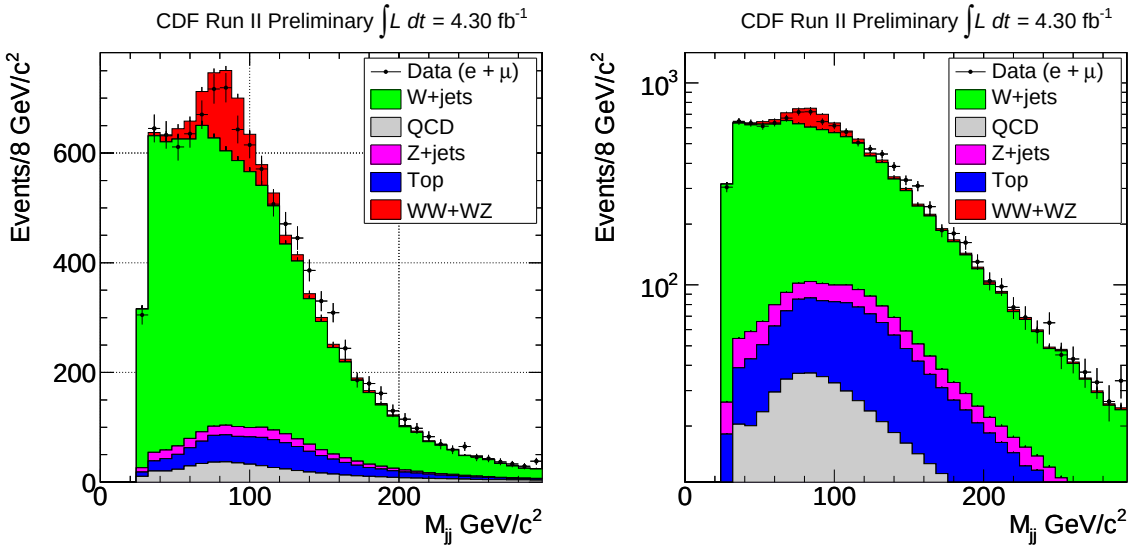

Figure 6: Expected M_{jj} distribution overimposed to data for the same of electrons and muons. Right: the same in log scale.

11 Background Modeling Studies

To test the MC accuracy and make sure that a possible resonance is not due to any particular mismodeling, we look at different physical regions of the di -jet spectrum. We apply different selection criteria to enhance each of our backgrounds and then verify data MC agreement

- **Excess sidebands**: $Mjj < 120$ and $Mjj > 160$. Fig. 7 - 11 show several kinematical distributions of muon sidebands. Fig. 30 - 34 show the corresponding distributions for electrons. We do not observe any significant disagreement with the exception of ΔR between the two jets. This discrepancy will be discussed in more detail in Section 14.

- **Events with two leptons to test $Z + jets$ in muons**: in addition to the missing E_T and the high P_T lepton we require another loosely identified lepton (including a high-momentum track with no other tracks nearby). Fig. 25- 29 show the kinematical distribution for muons. A good agreement is observed. The same test is not meaningful for electrons and will not be shown.

- $N_{jet} \geq 3$ **to enhance the top background**. Fig. 14- 18 show the kinematical distribution for muons and Fig. 37-41 for electrons.

- $N_{jet} \geq 4$, again to enhance the top contribution . Fig. 19- 23 show the kinematical distribution for muons and Fig. 42-46 for electrons.

- **W + jets**: testing W+jets is not trivial because it is not characterized by a distinguished signature. More stringent tests will be discussed in Section 13 However, we can check that the MC reproduces the W+jets cross sections. We look at the 2nd jet E_T distribution when there are just two jets in the event, at the 3rd jet E_T when there are exactly three jets in the event and at the 4th jet E_T when there are exactly four jets in the event. These distributions are shown in Fig. 24 for muons and fig. 47 for electrons. In all cases there is good agreement between data and MC.

In the following plots, the error band is determined by the QCD fit of Sec.9 only. No systematic uncertainties is included at this time.

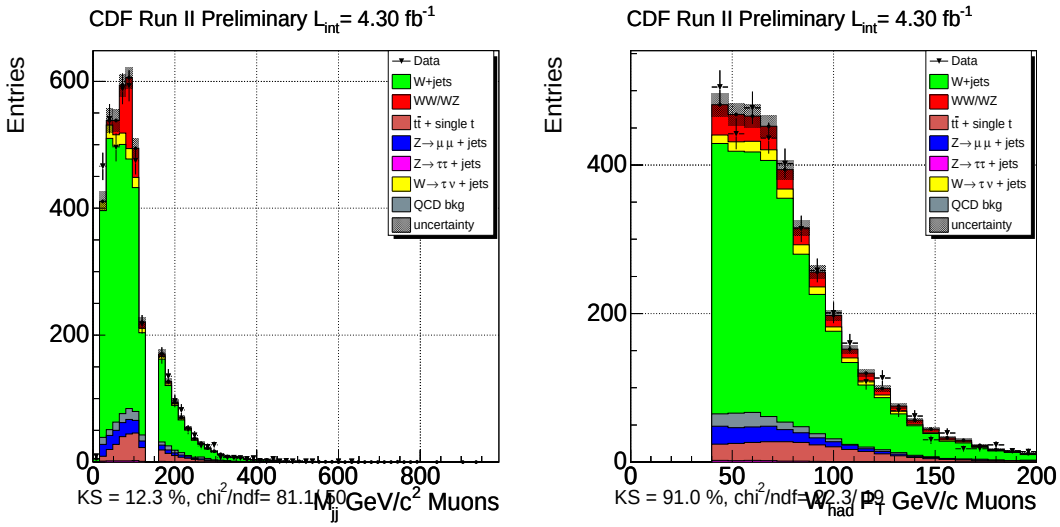

Figure 7: Left: M_{jj} for excess sidebands. Right: W P_T for excess sidebands

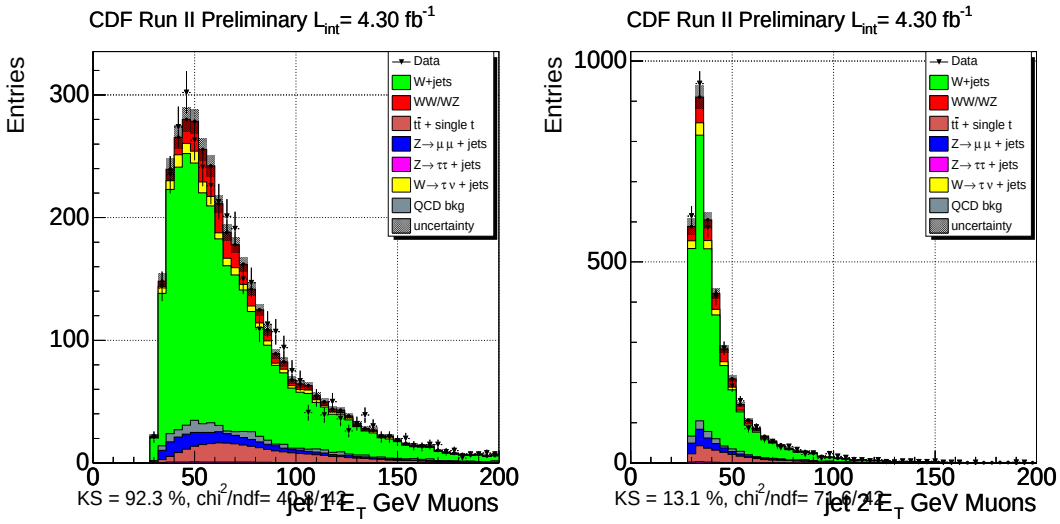

Figure 8: Left: jet 1 E_T for excess sidebands. Right: jet 2 E_T for excess sidebands

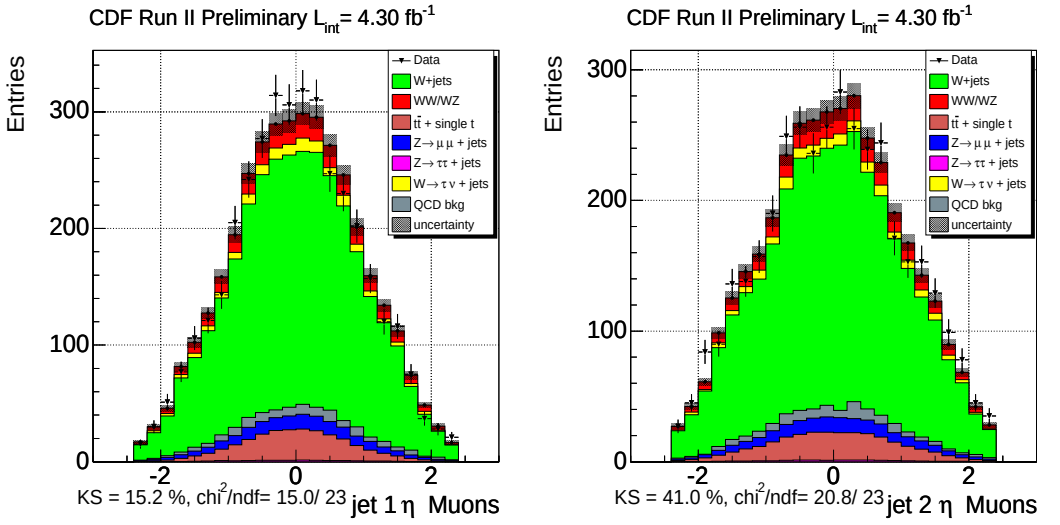

Figure 9: Left: jet 1 η for excess sidebands. Right: jet 2 η for excess sidebands

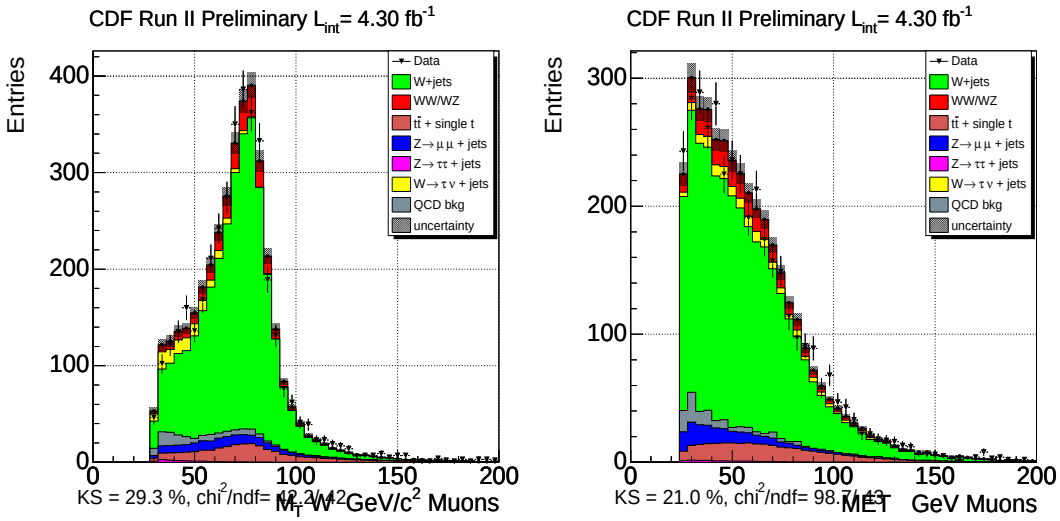

Figure 10: Left: m_T W for excess sidebands. Right: $\not\!\!E_T$ for excess sidebands

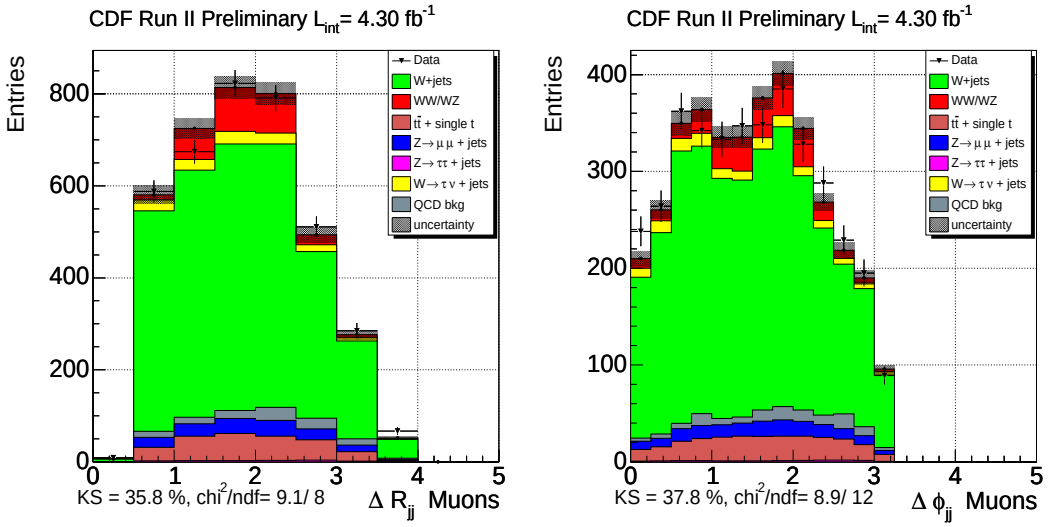

Figure 11: Left: ΔR_{jj} W for excess sidebands. Right: $\Delta\phi_{jj}$ for excess sidebands

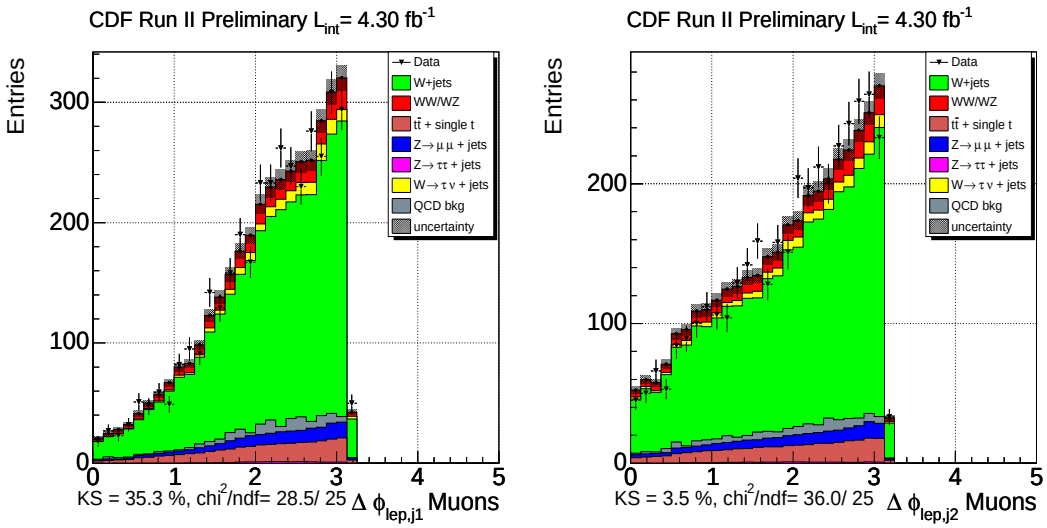

Figure 12: Left: $\Delta\phi_{lep,j1}$ W for excess sidebands. Right: $\Delta\phi_{lep,j2}$ for excess sidebands

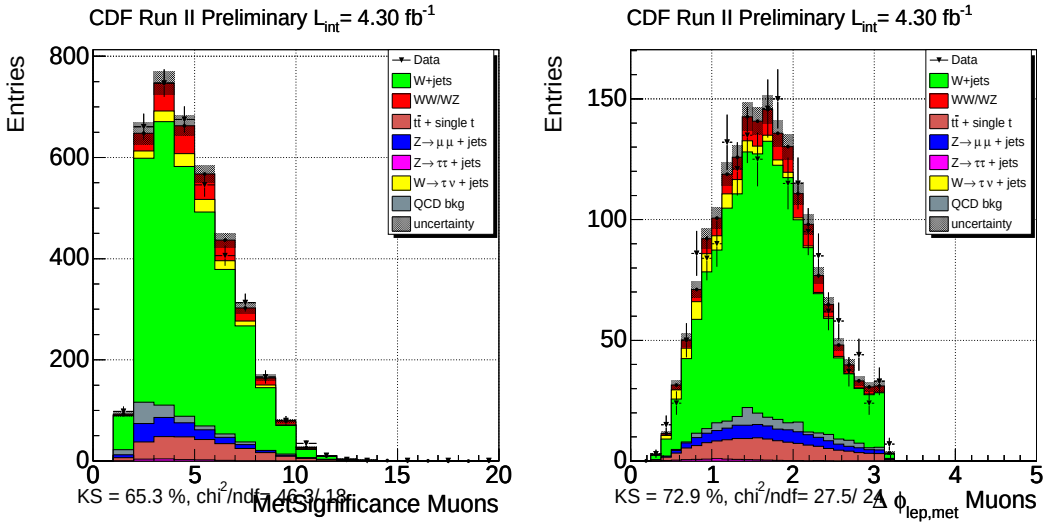

Figure 13: Left: Met significance for excess sidebands. Right: $\Delta\phi_{lep,met}$ for excess sidebands

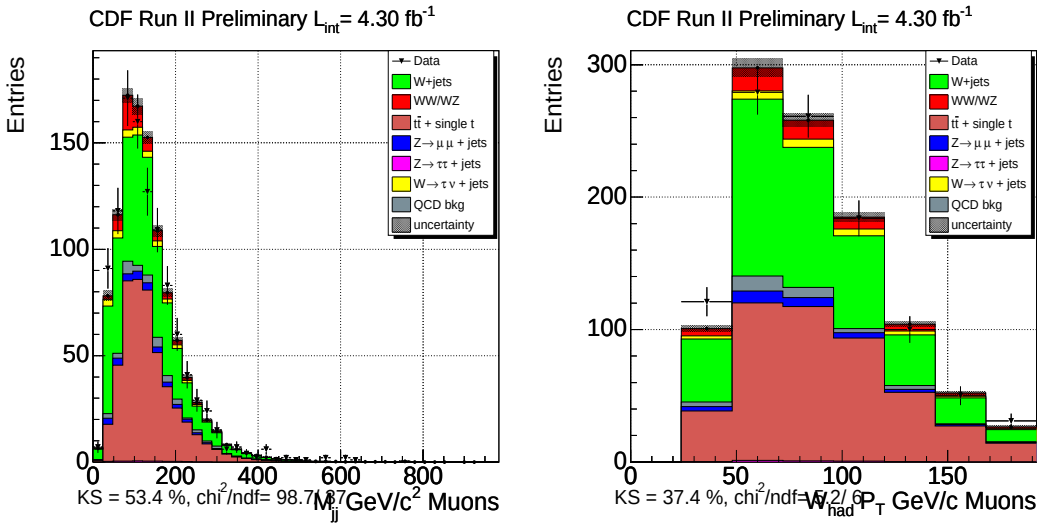

Figure 14: Left: M_{jj} for events with >= 3 jet. Right: W P_T for events with >= 3 jet

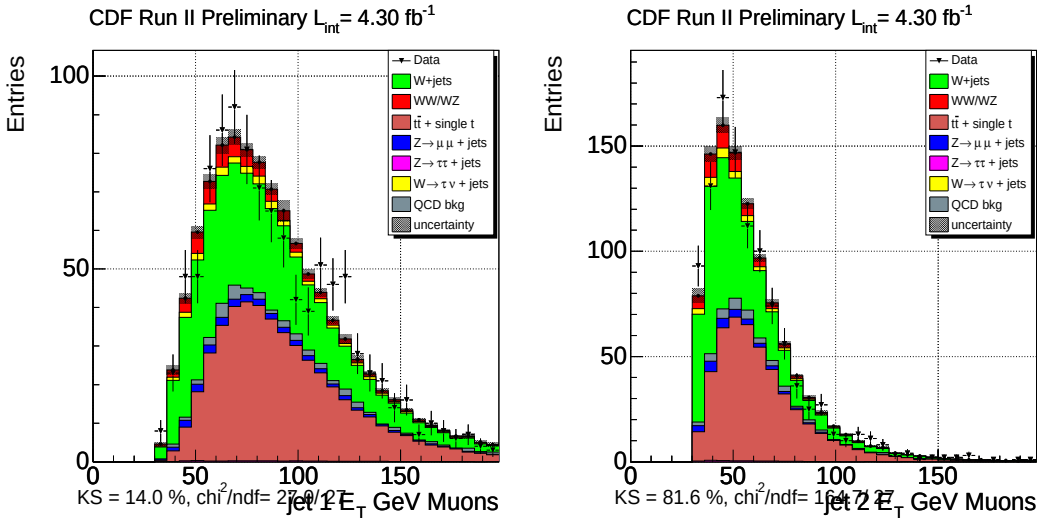

Figure 15: Left: jet 1 E_T for events with >= 3 jet. Right: jet 2 E_T for events with >= 3 jet

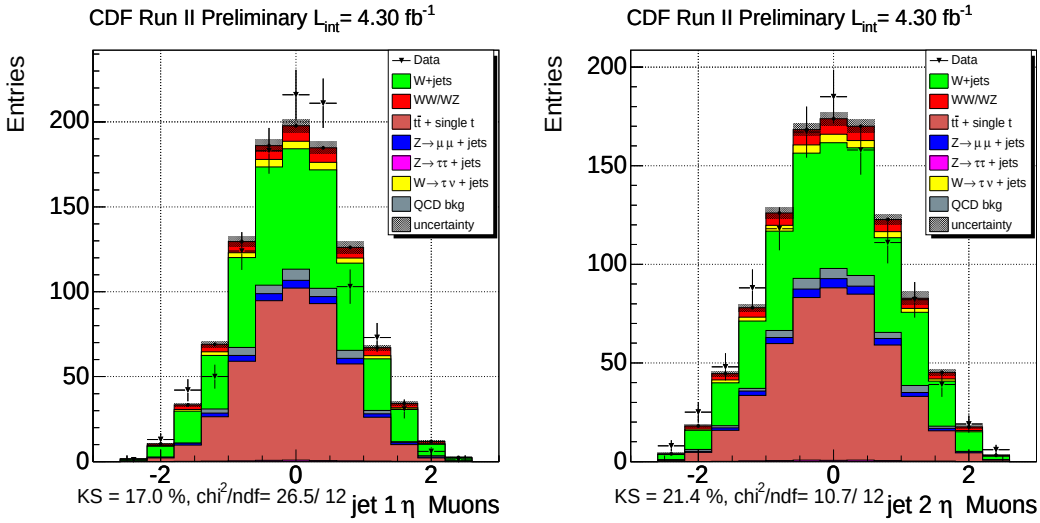

Figure 16: Left: jet 1 η for events with >= 3 jet. Right: jet 2 η for events with >= 3 jet

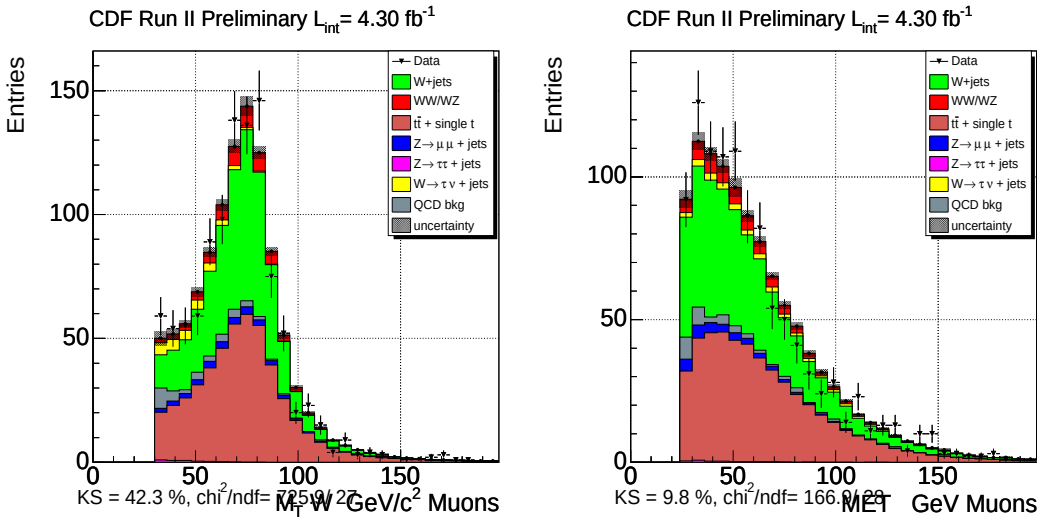

Figure 17: Left: m_T W for events with >= 3 jets. Right: $\not\!\!E_T$ for events with >= 3 jet

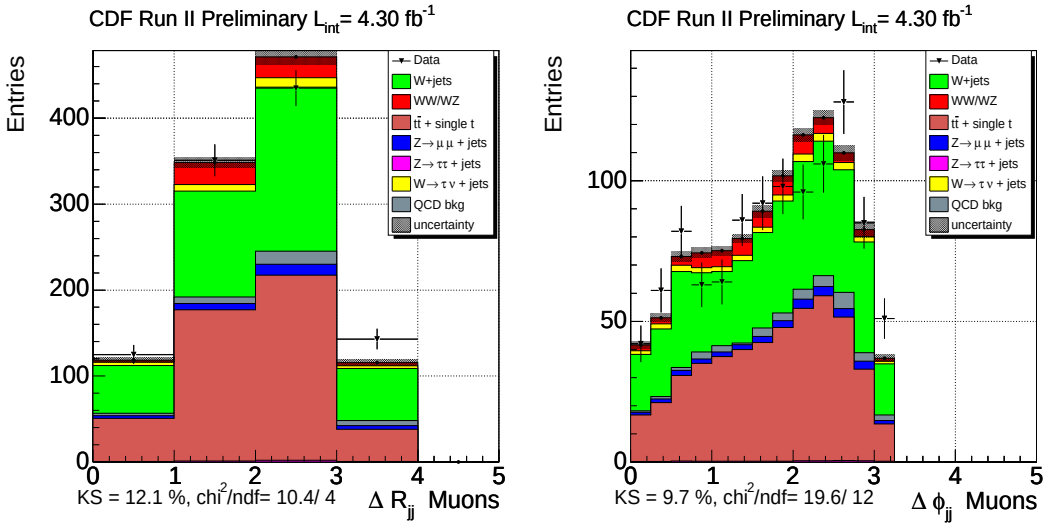

Figure 18: Left: ΔR_{jj} for events with >= 3 jets. Right: $\Delta\phi_{jj}$ for events with >= 3 jets

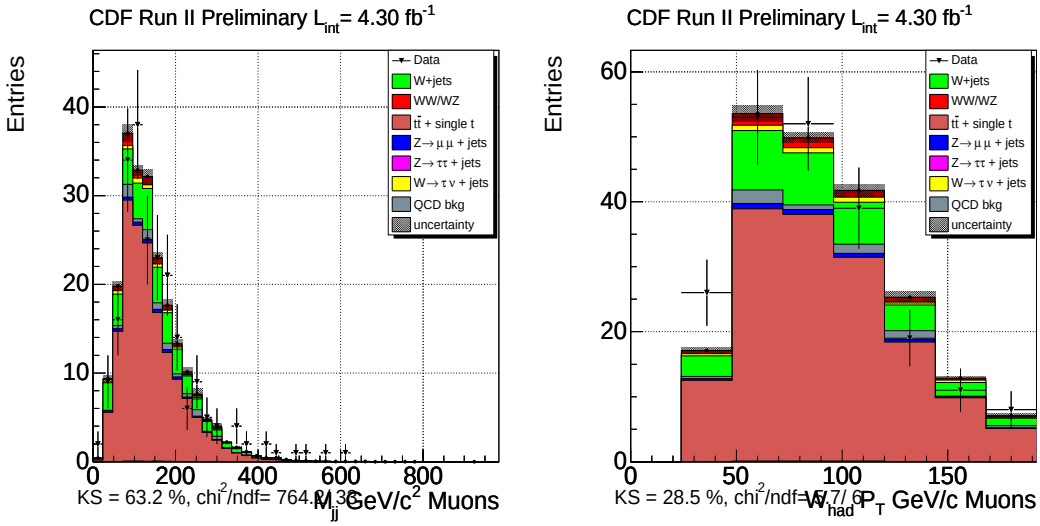

Figure 19: Left: M_{jj} for events with >= 4 jet. Right: W P_T for events with >= 4 jet

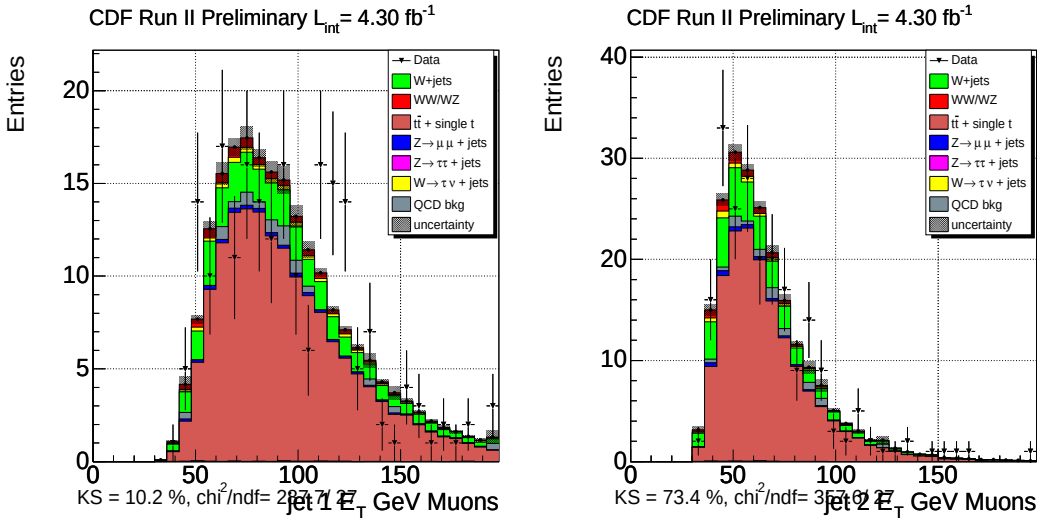

Figure 20: Left: jet 1 E_T for events with >= 4 jet. Right: jet 2 E_T for events with >= 4 jet

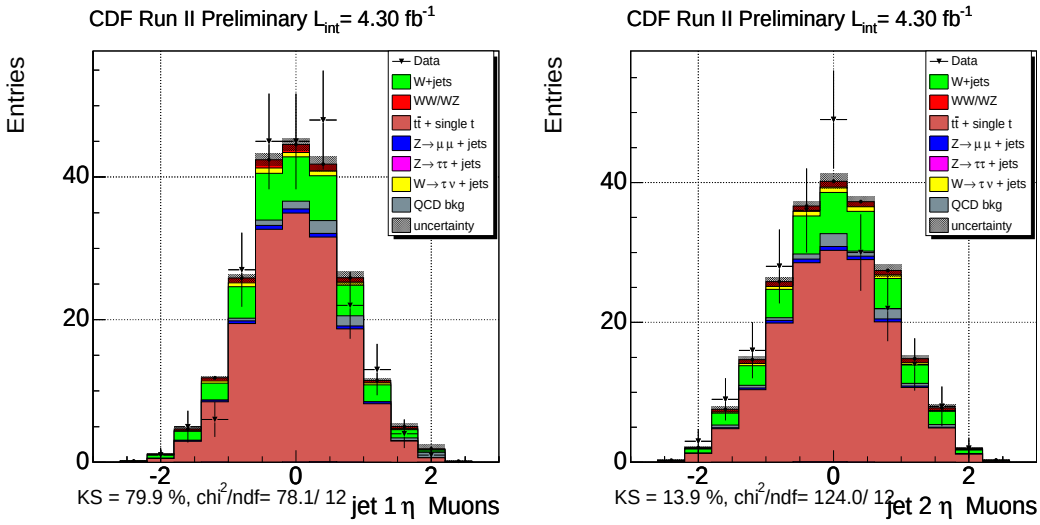

Figure 21: Left: jet 1 η for events with >= 4 jet. Right: jet 2 η for events with >= 4 jet

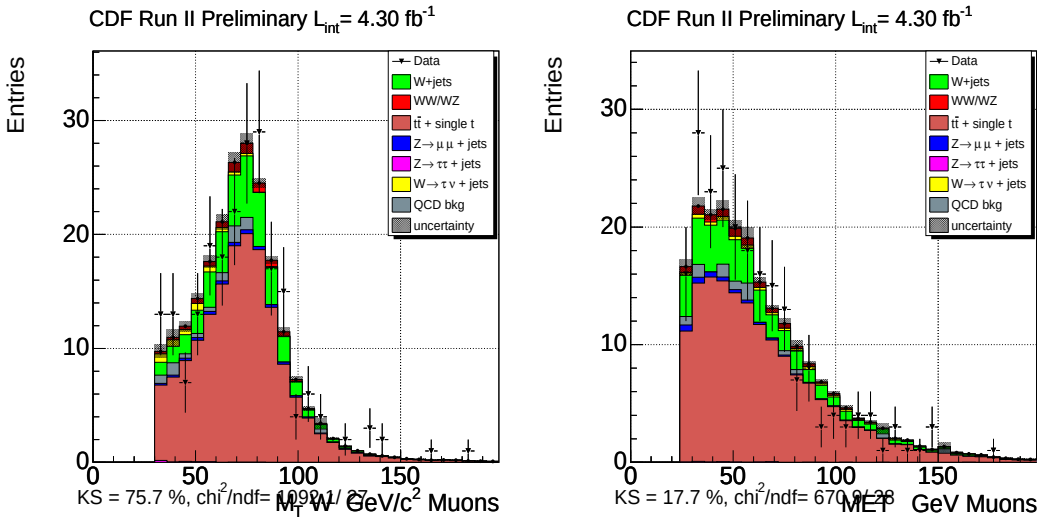

Figure 22: Left: m_T W for events with >= 4 jets. Right: $\not\!\!E_T$ for events with >= 4 jet

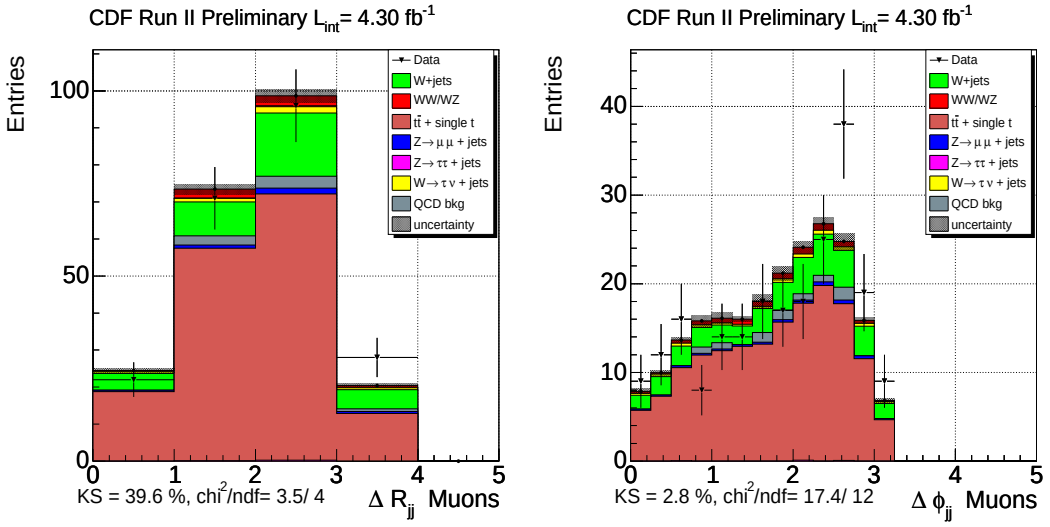

Figure 23: Left: ΔR_{jj} for events with >= 4 jets. Right: $\Delta\phi_{jj}$ for events with >= 4 jets

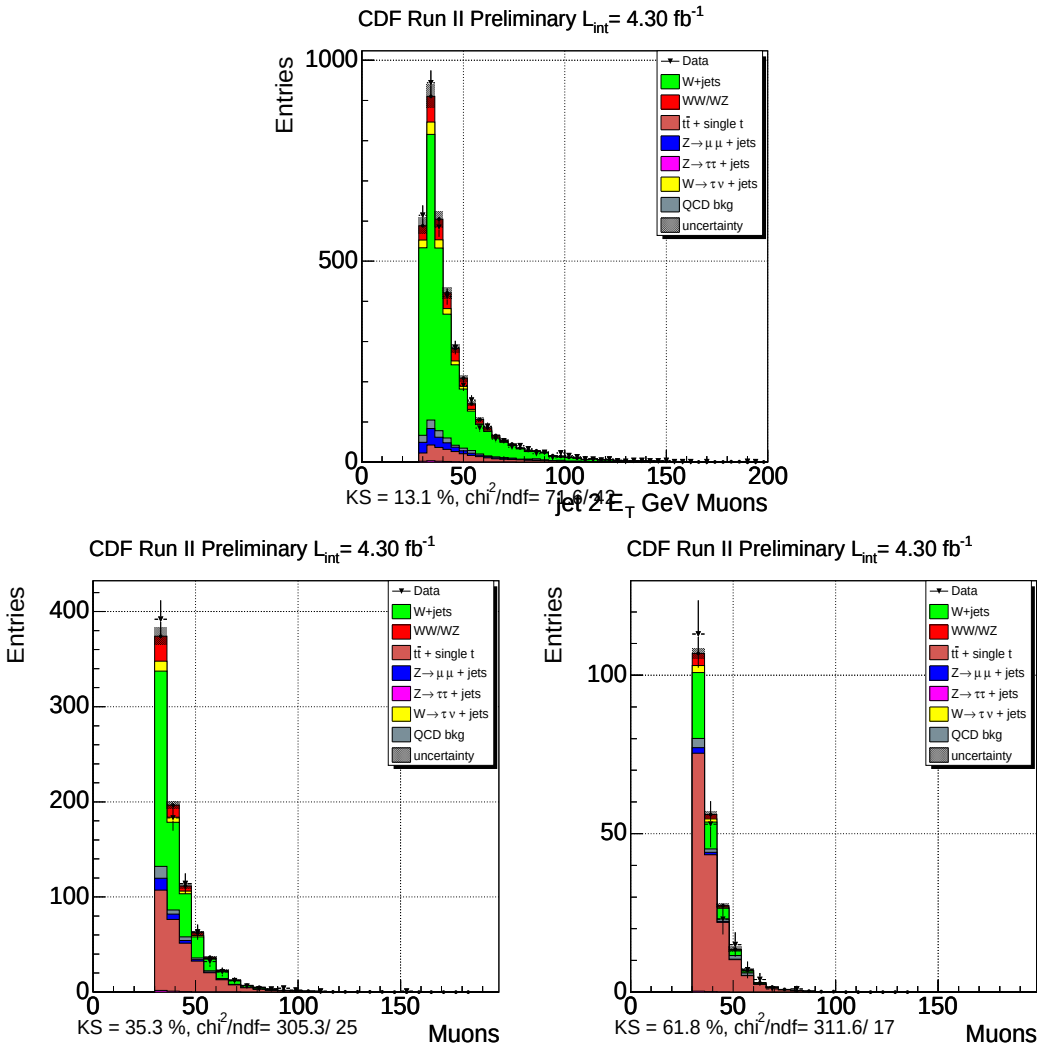

Figure 24: Top: jet 2 E_T for events with 2 jets. bottom. Bottom left: jet 3 E_T for events with 3 jets. Bottom right: jet 4 E_T for events with 4 jets.

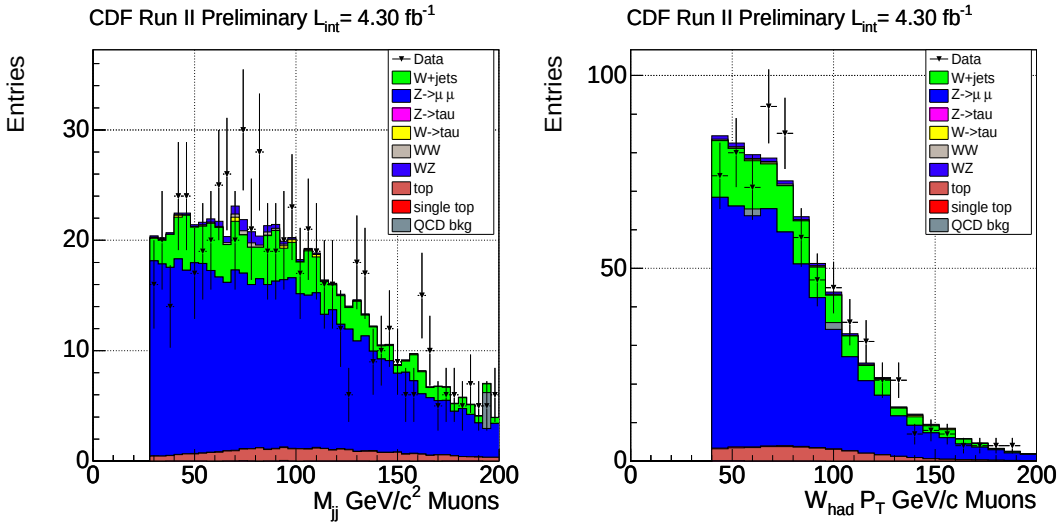

Figure 25: Left: M_{jj} for events with another lepton. Right: W P_T for events with another lepton

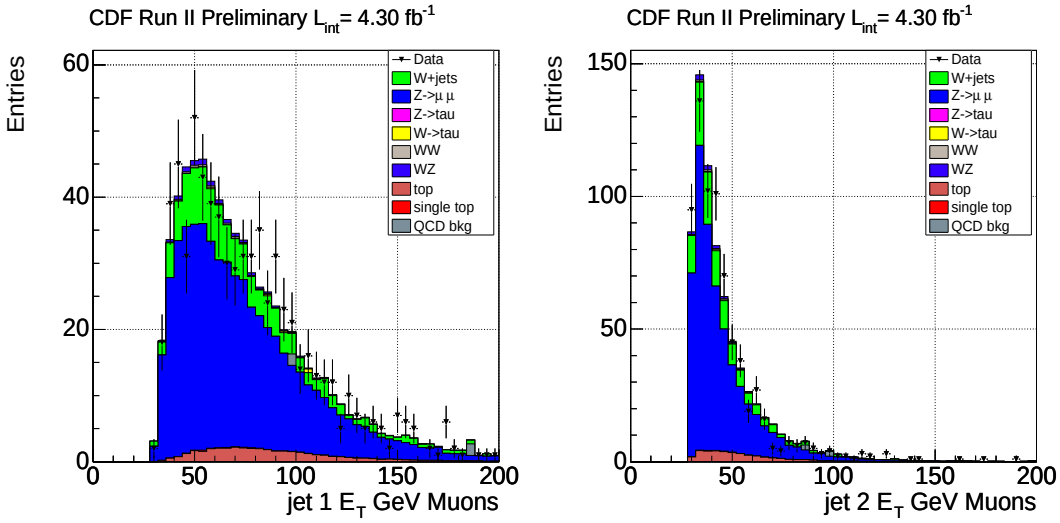

Figure 26: Left: jet 1 E_T for events with another lepton. Right: jet 2 E_T for events with another lepton

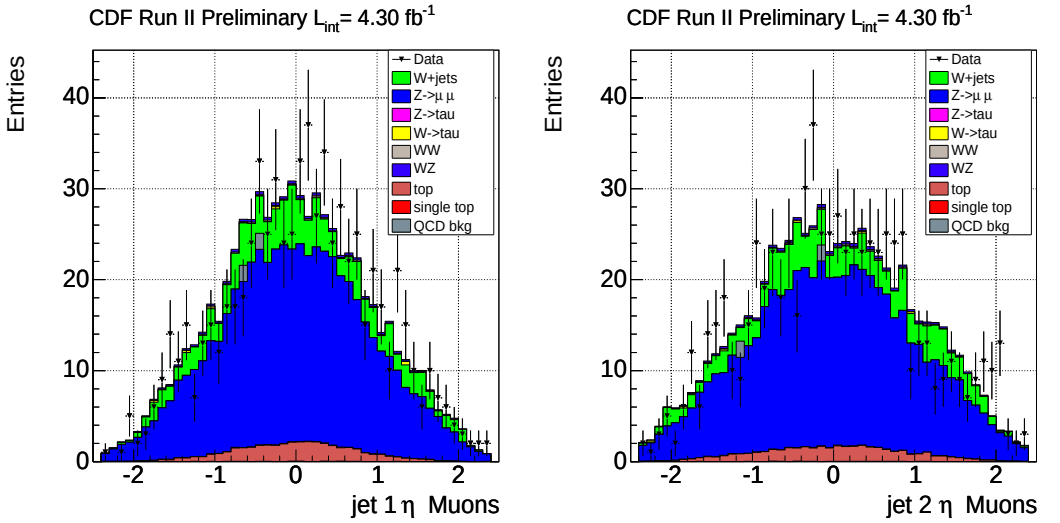

Figure 27: Left: jet 1 η for events with another lepton. Right: jet 2 η for events with another lepton

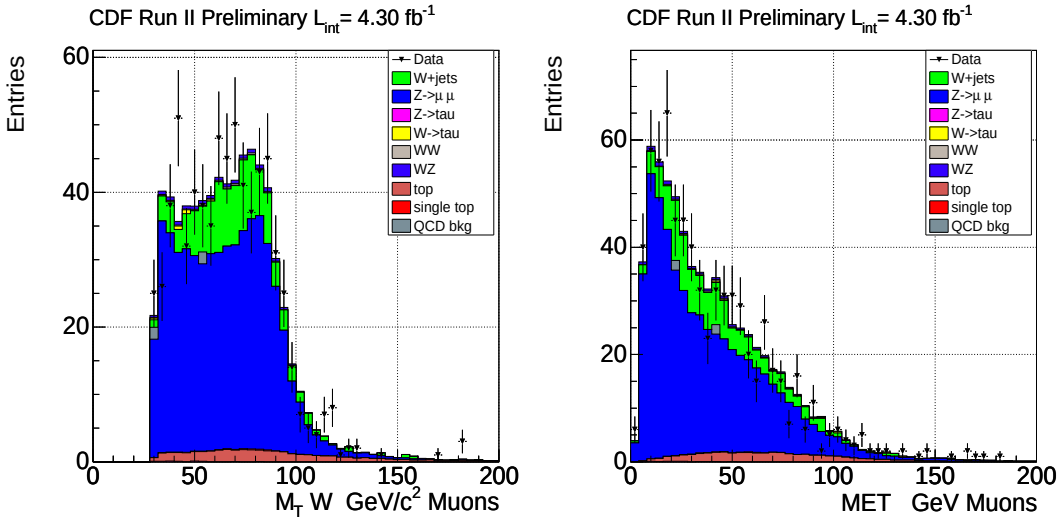

Figure 28: Left: m_T W for events with another lepton. Right: $\not\!\!E_T$ for events with another lepton

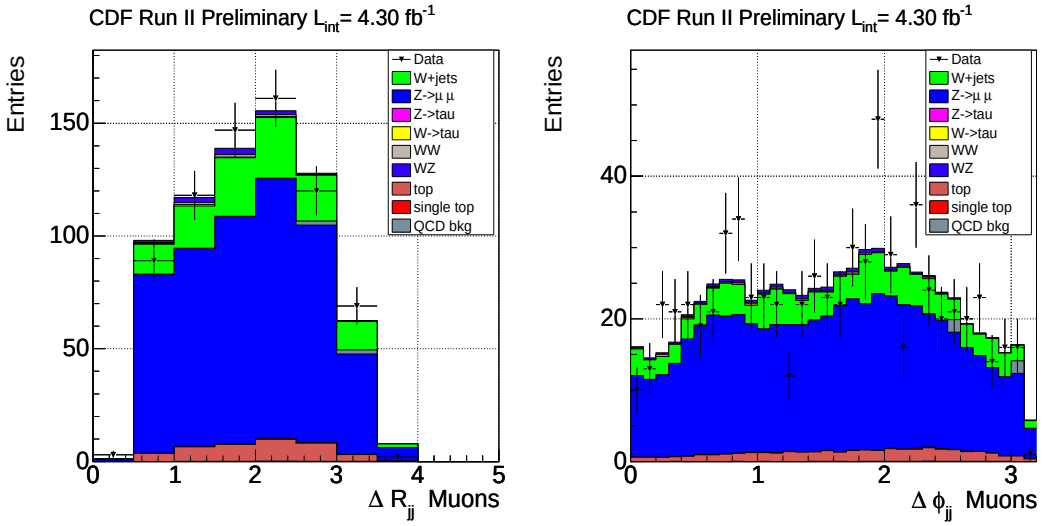

Figure 29: Left: ΔR_{jj} for events with another lepton. Right: $\Delta\phi_{jj}$ for events with another lepton

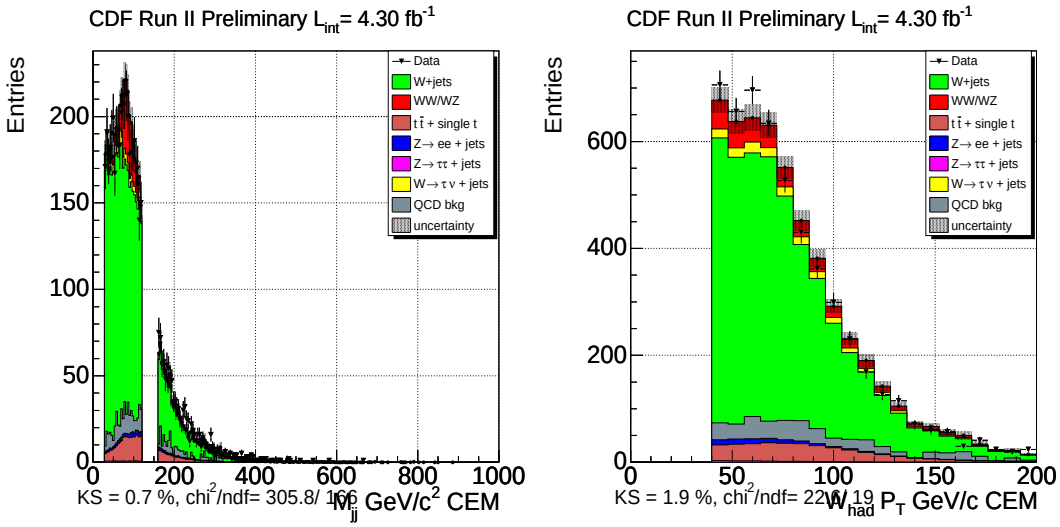

Figure 30: Left: M_{jj} for excess sidebands. Right: W P_T for excess sidebands

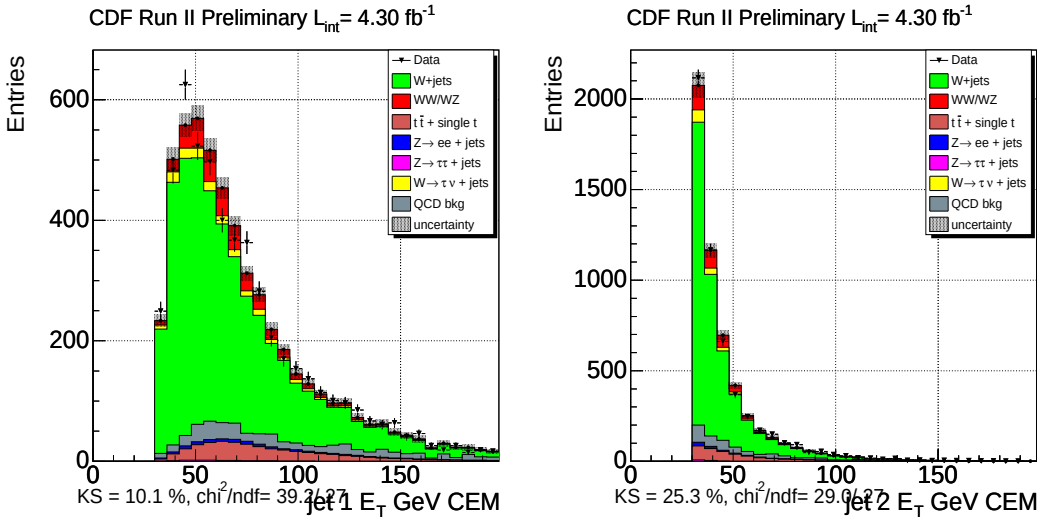

Figure 31: Left: jet 1 E_T for excess sidebands. Right: jet 2 E_T for excess sidebands

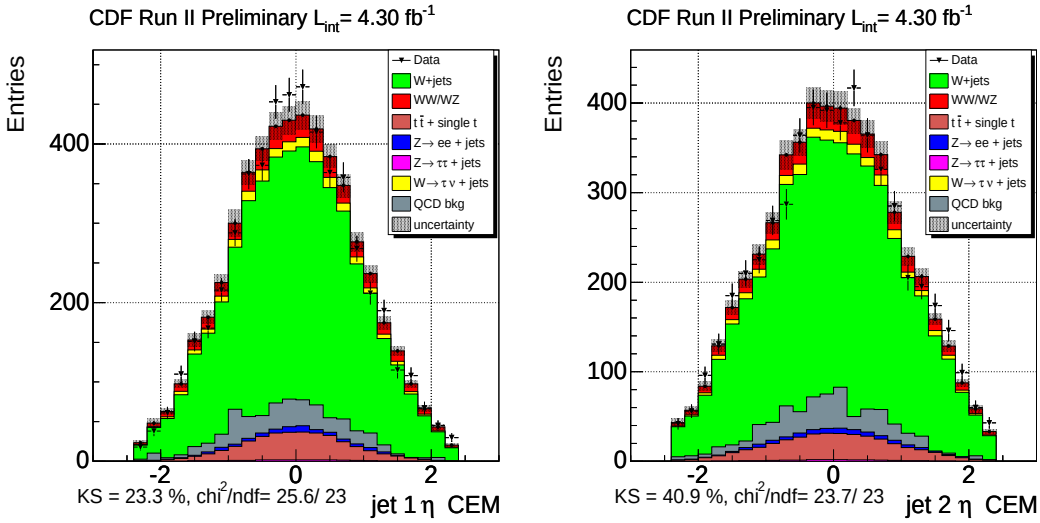

Figure 32: Left: jet 1 η for excess sidebands. Right: jet 2 η for excess sidebands

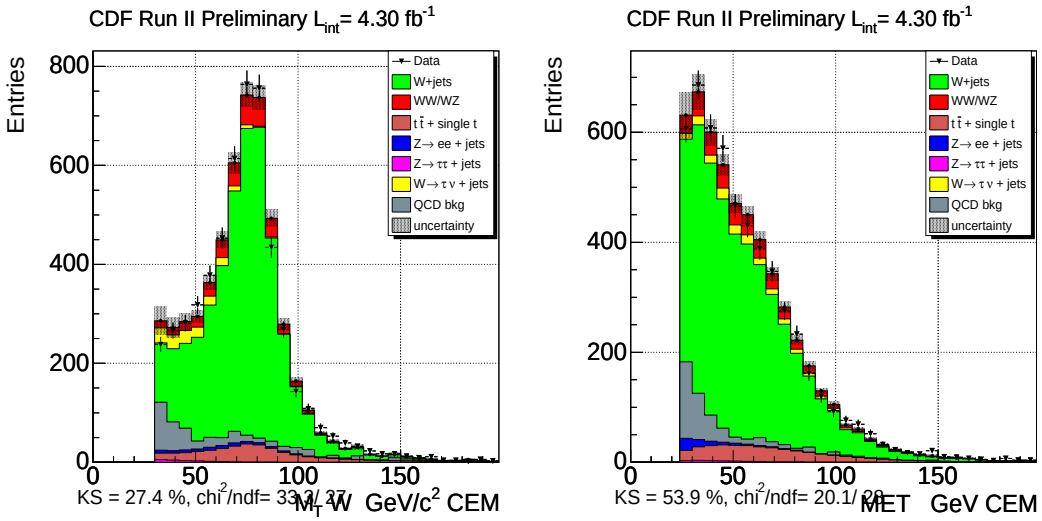

Figure 33: Left: m_T W for excess sidebands. Right: $\not\!\!E_T$ for excess sidebands

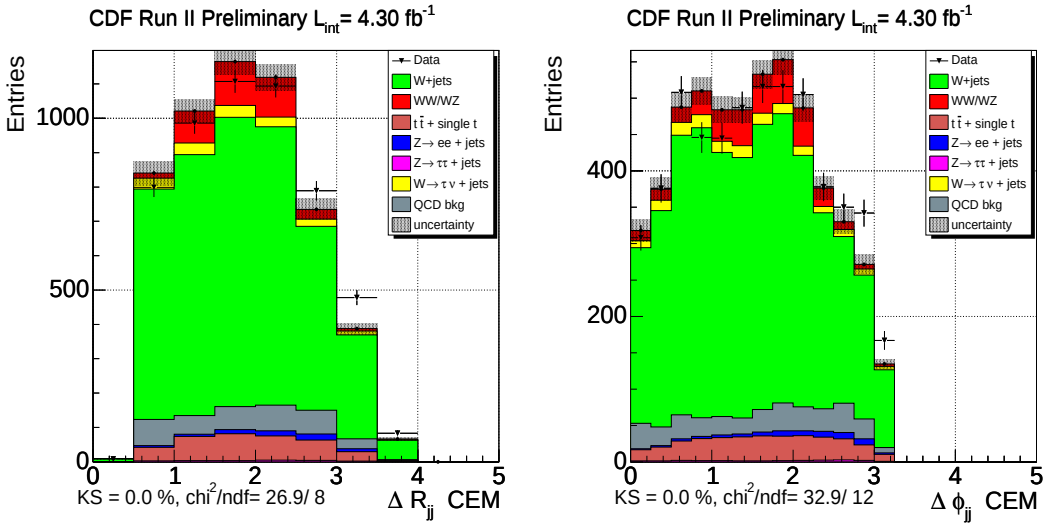

Figure 34: Left: ΔR_{jj} W for excess sidebands. Right: $\Delta\phi_{jj}$ for excess sidebands

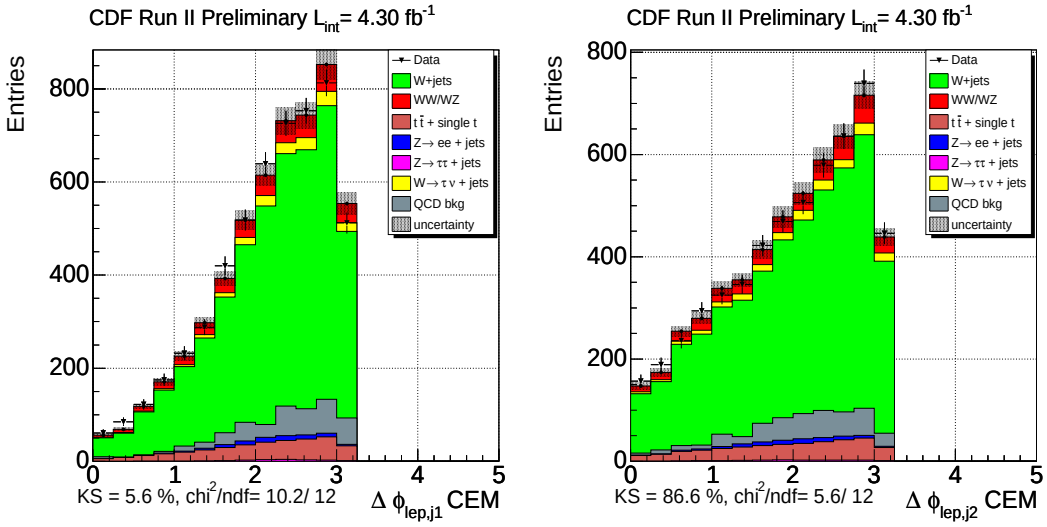

Figure 35: Left: $\Delta\phi_{lep,j1}$ W for excess sidebands. Right: $\Delta\phi_{lep,j2}$ for excess sidebands

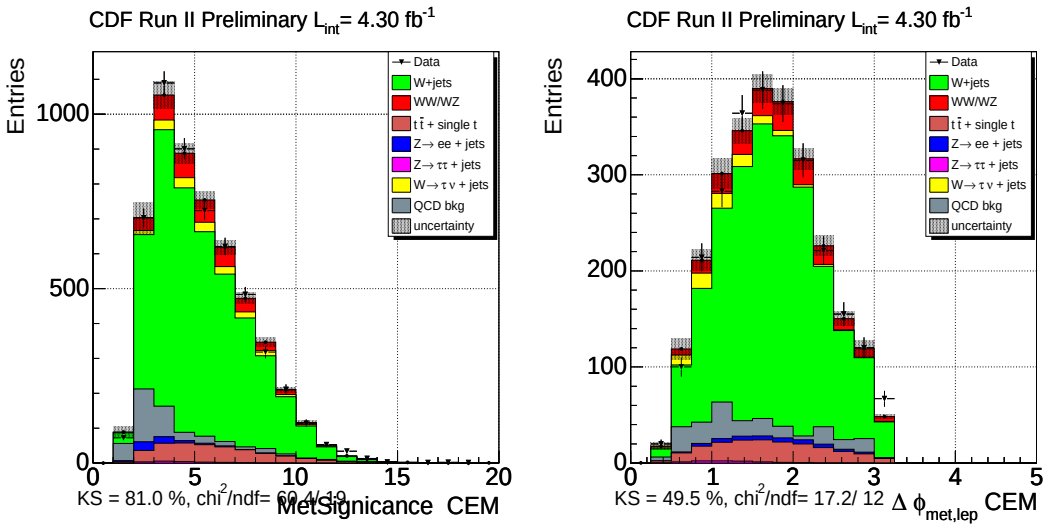

Figure 36: Left: Met significance for excess sidebands. Right: $\Delta\phi_{lep,met}$ for excess sidebands

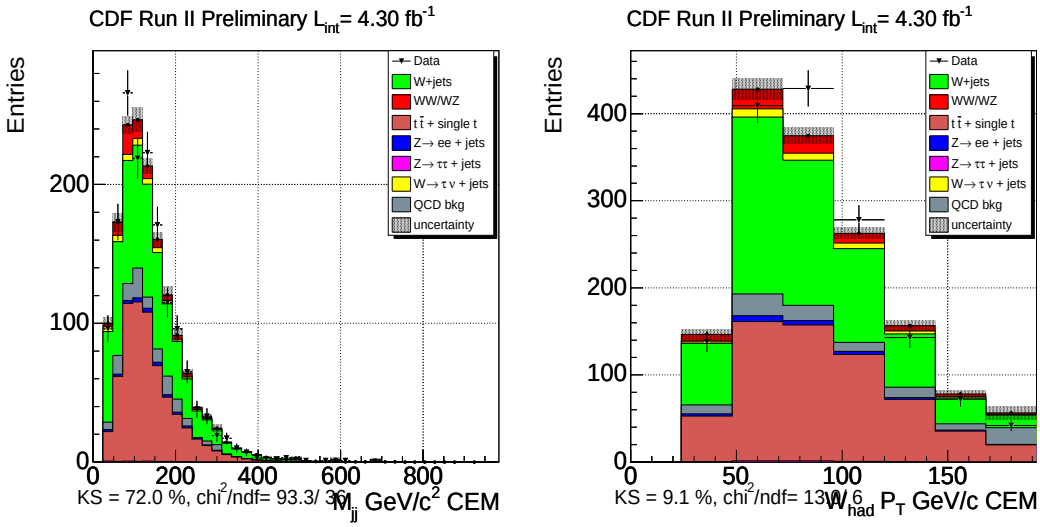

Figure 37: Left: M_{jj} for events with >= 3 jet. Right: W P_T for events with >= 3 jet

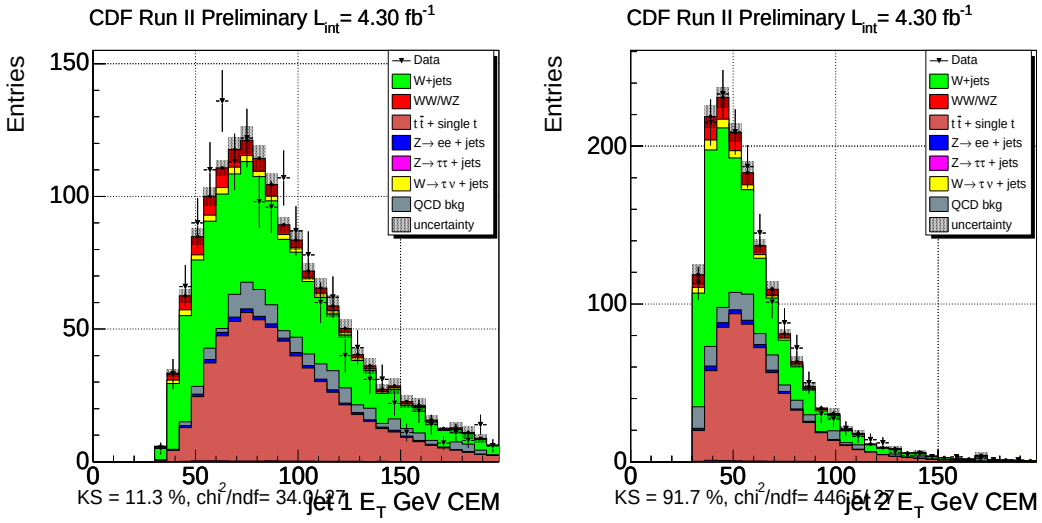

Figure 38: Left: jet 1 E_T for events with >= 3 jet. Right: jet 2 E_T for events with >= 3 jet

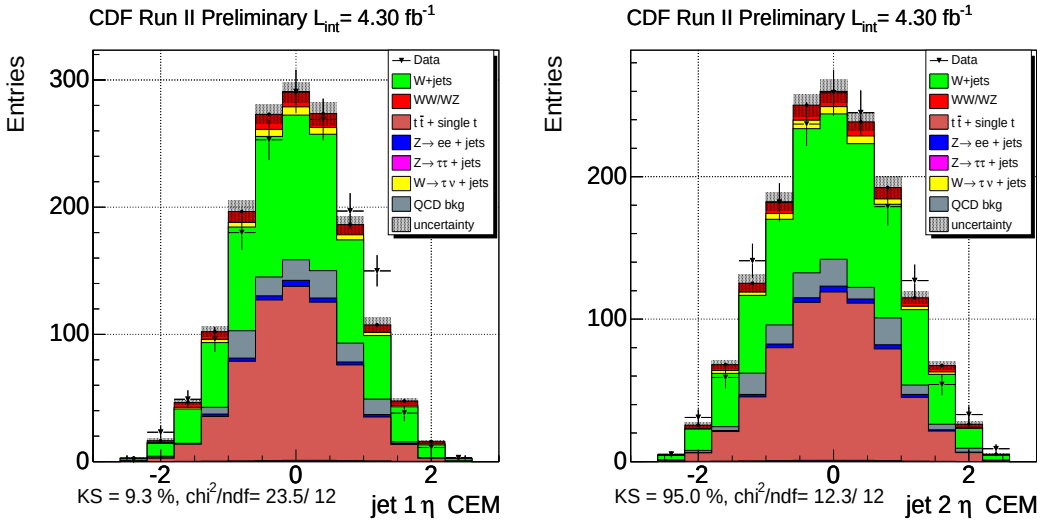

Figure 39: Left: jet 1 η for events with >= 3 jet. Right: jet 2 η for events with >= 3 jet

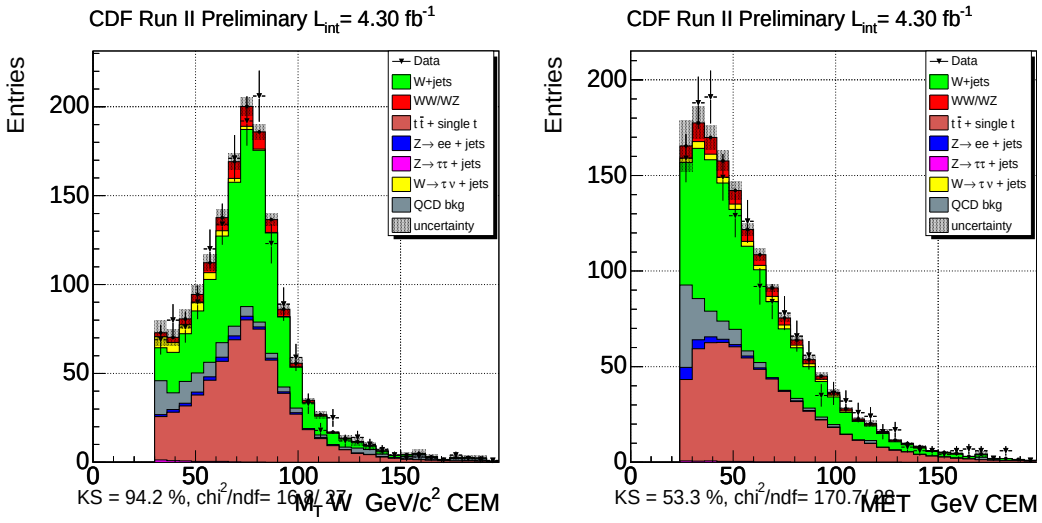

Figure 40: Left: m_T W for events with >= 3 jets. Right: $\not\!\!E_T$ for events with >= 3 jet

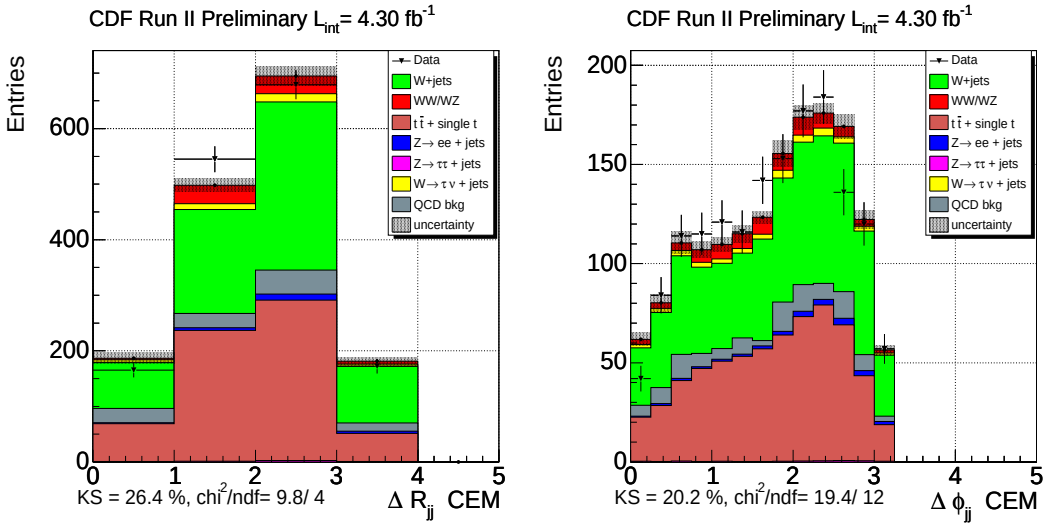

Figure 41: Left: ΔR_{jj} for events with >= 3 jets. Right: $\Delta\phi_{jj}$ for events with >= 3 jets

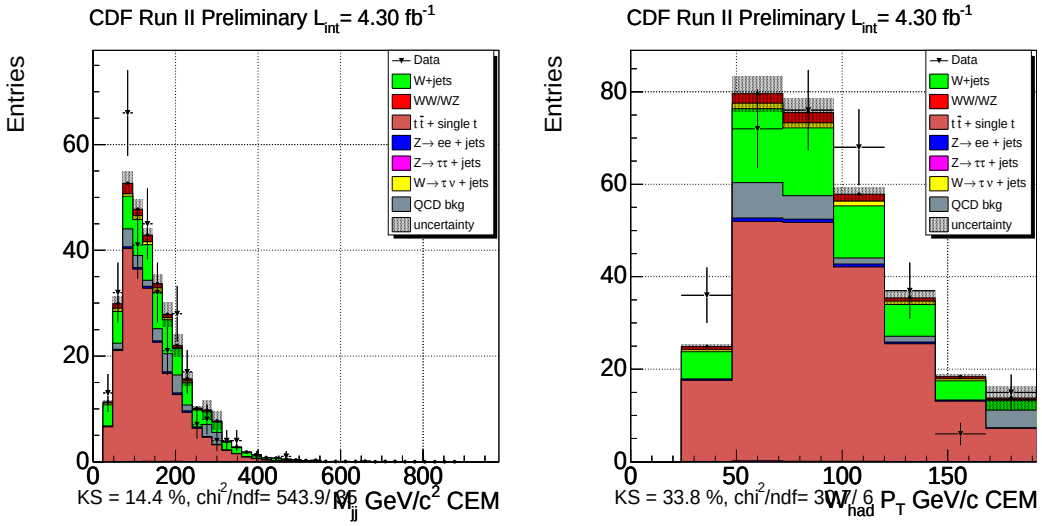

Figure 42: Left: M_{jj} for events with >= 4 jet. Right: W P_T for events with >= 4 jet

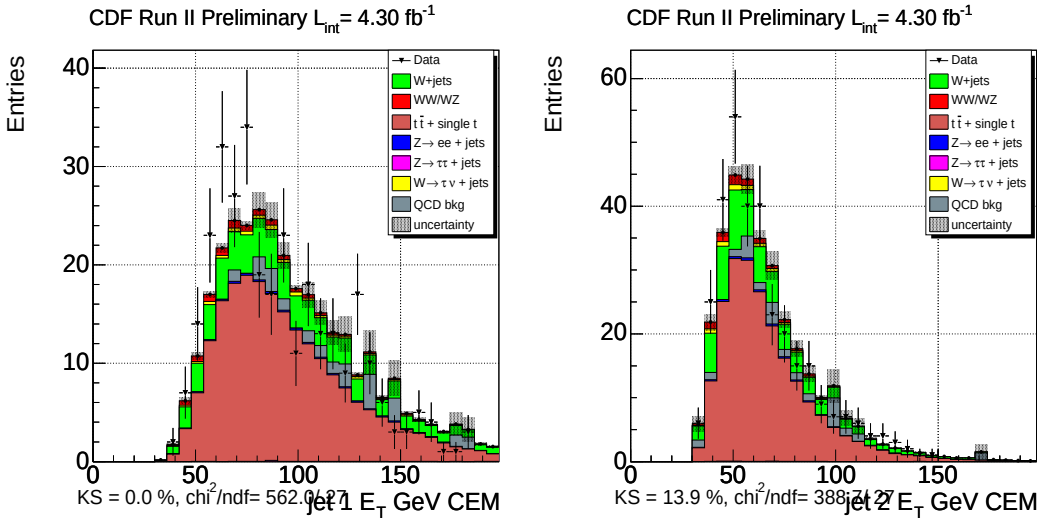

Figure 43: Left: jet 1 E_T for events with >= 4 jet. Right: jet 2 E_T for events with >= 4 jet

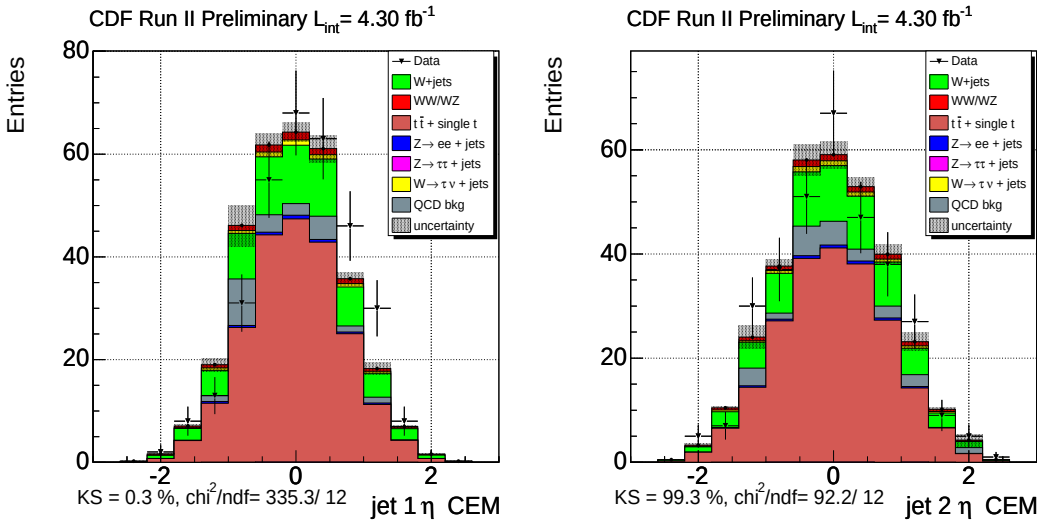

Figure 44: Left: jet 1 η for events with >= 4 jet. Right: jet 2 η for events with >= 4 jet

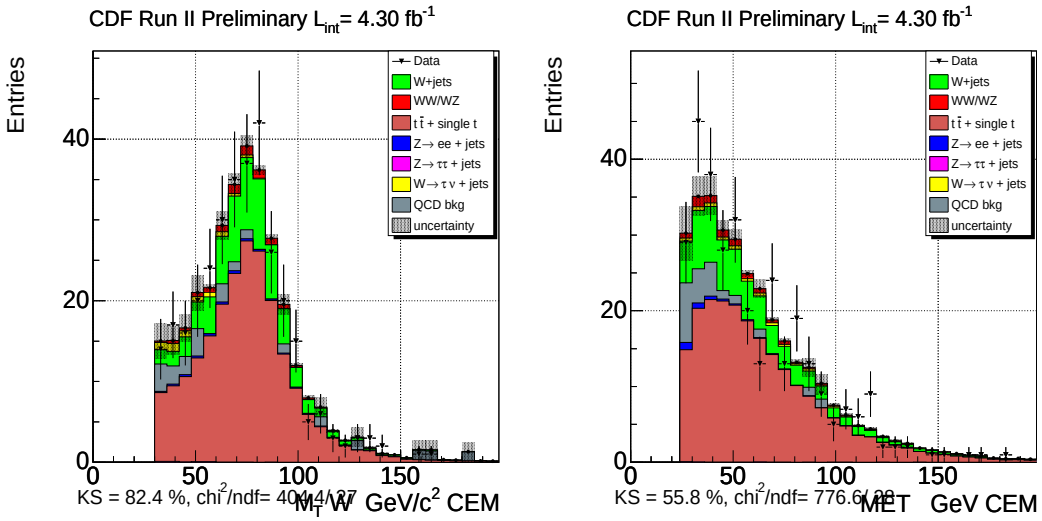

Figure 45: Left: m_T W for events with >= 4 jets. Right: $\not\!\!E_T$ for events with >= 4 jet

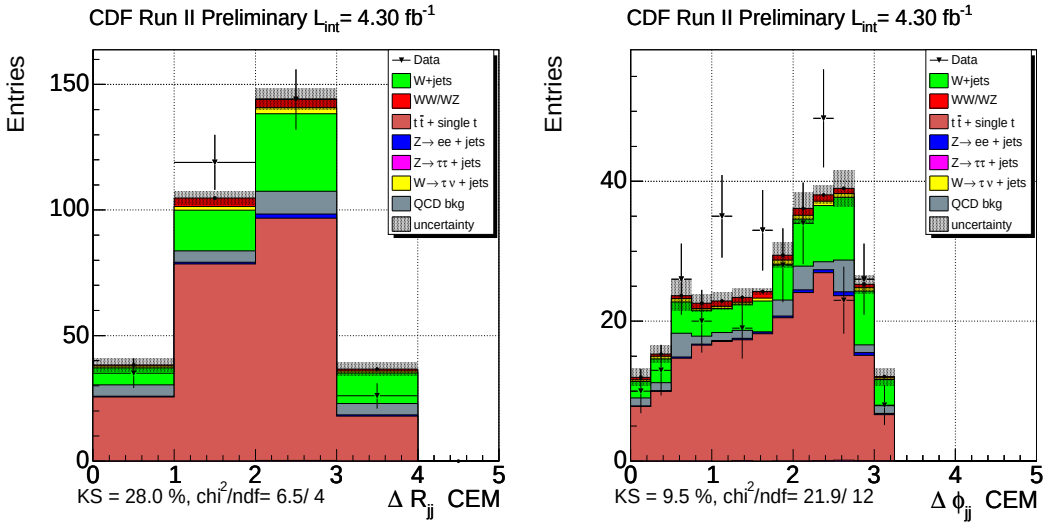

Figure 46: Left: ΔR_{jj} for events with >= 4 jets. Right: $\Delta\phi_{jj}$ for events with >= 4 jets

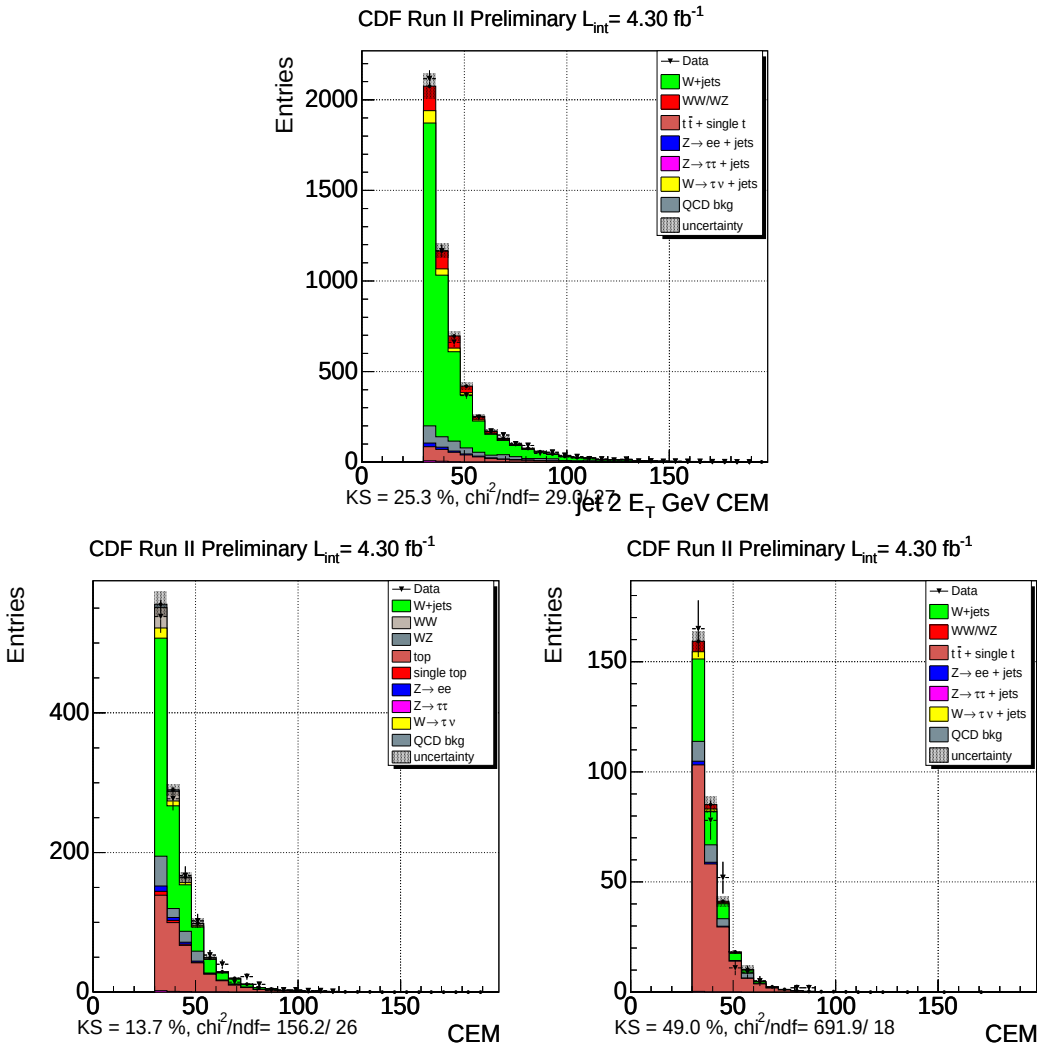

Figure 47: Top: jet 2 E_T for events with 2 jets. bottom. Bottom left: jet 3 E_T for events with 3 jets. Bottom right: jet 4 E_T for events with 4 jets.

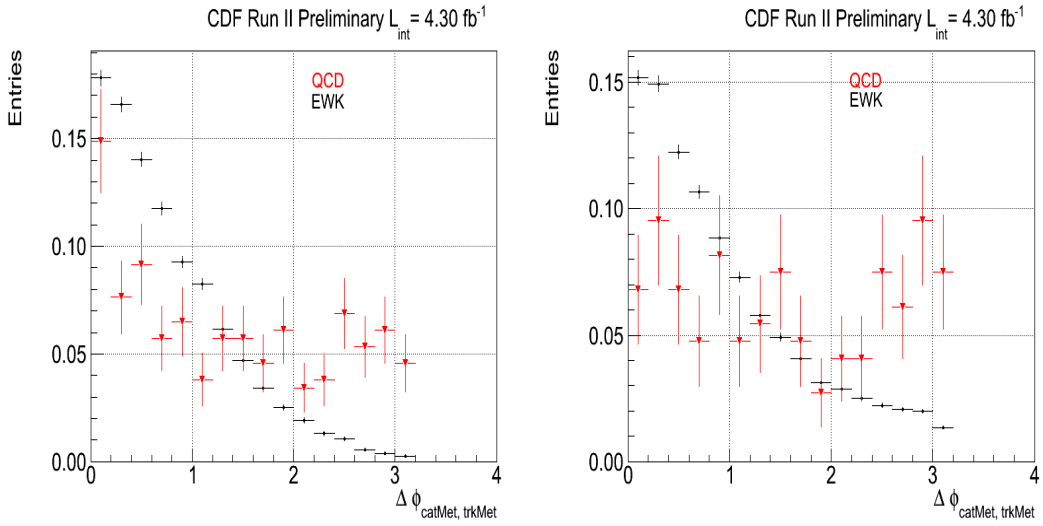

Figure 48: Left: $\Delta\phi(\not\!\!P_T, \not\!\!E_T)$ for EWK (black) and QCD (red) backgrounds in the muon sample. Right: $\Delta\phi(\not\!\!P_T, \not\!\!E_T)$ for EWK (black) and QCD (red) backgrounds in the electron sample. Plots are nomalized to unit area.

12 Multijet QCD: additional studies

We further investigate the multijet QCD background by considering additional variables whose distribution is expected to be different for QCD and EWK.
At first, we consider the angle $\Delta\phi(\not\!\!P_T, \not\!\!E_T)$ in the transverse plane between the solely calorimetric $\not\!\!E_T$ and the transverse missing momentum evaluated using tracks ($\not\!\!P_T$). As shown in Fig.48, $\Delta\phi(\not\!\!P_T, \not\!\!E_T)$ peaks at low values for the EWK component, while it is almost flat along the spectrum and slightly peaking at high values in QCD.
In Fig.49, we compare $\Delta\phi(\not\!\!P_T, \not\!\!E_T)$ between data and our background model. The error band includes the statistical uncertainty obtained by the $\not\!\!E_T$ fits of Sec.9. Within uncertainties, we observe a very good agreement between data and expectation, supporting our estimate of the small QCD contribution.

Another variable characterized by discriminating power between EWK and QCD is the $\Delta\phi(\not\!\!E_T, closest - jet)$, defined as the angle in the transverse plane between $\not\!\!E_T$ and the closest jet with raw $E_T > 5GeV$.
A shown in Fig.50, QCD tends to peak sharply at low $\Delta\phi(\not\!\!E_T, closest - jet)$ while EWK has a wider distribution with a broad peak at high $\Delta\phi(\not\!\!E_T, closest - jet)$. In our sample, this variable seems to have better separation power than $\Delta\phi(\not\!\!P_T, \not\!\!E_T)$.
In Fig.51, we compare $\Delta\phi(\not\!\!E_T, closest - jet)$ between data and our background model. Again, the error band includes the statistical uncertainty on the QCD and W+jet obtained by the $\not\!\!E_T$ fits of Sec.9. Within uncertainties, we observe a very good agreement between data and expectation also for $\Delta\phi(\not\!\!E_T, closest - jet)$.

The quality of our QCD fits of Sec. 9 combined with the almost independent

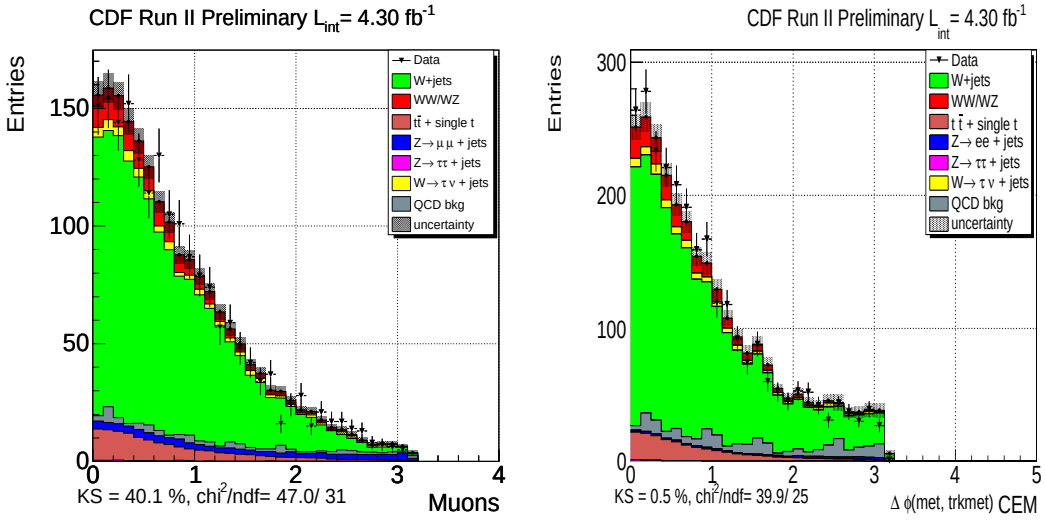

Figure 49: Left: $\Delta\phi(\not\!\!P_T, \not\!\!E_T)$ in the muon sample. Right: $\Delta\phi(\not\!\!P_T, \not\!\!E_T)$ in the electron sample.

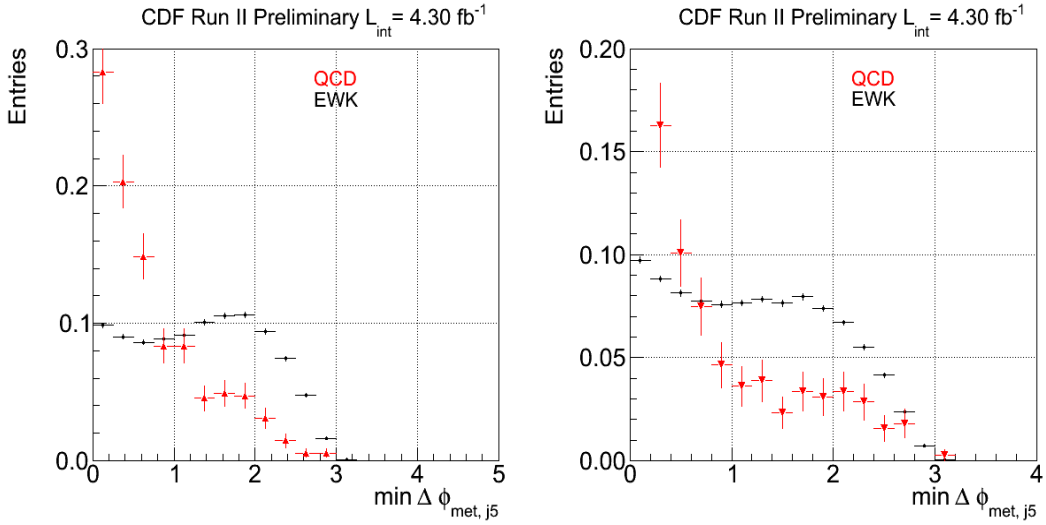

Figure 50: Left: $\Delta\phi(\not\!\!E_T, closest - jet)$ for EWK (black) and QCD (red) backgrounds in the muon sample. Right: $\Delta\phi(\not\!\!E_T, closest - jet)$ for EWK (black) and QCD (red) backgrounds in the electron sample. Plots are nomalized to unit area.

checks on $\Delta\phi(\not\!\!P_T, \not\!\!E_T)$ and $\Delta\phi(\not\!\!E_T, closest - jet)$ give us very good confidence in our estimation of the QCD contribution both in the electron and muon samples. In addition, the QCD fraction is gaussian constrained in the fit, i.e. allowed to move within the constraint.

We then look at the multijet QCD M_{jj} distribution to check how sensitive we are

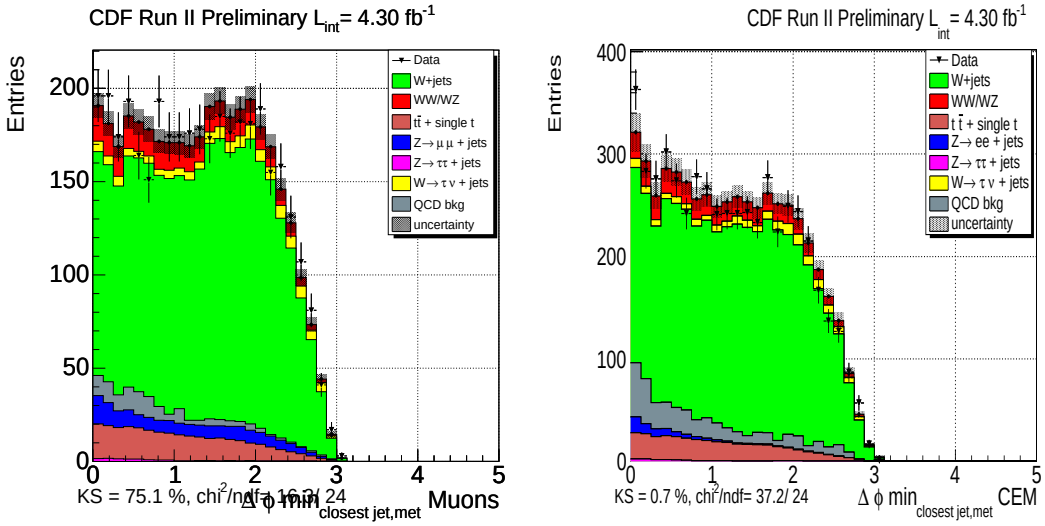

Figure 51: Left: $\Delta\phi(\not\!\!E_T, closest - jet)$ in the muon sample. Right: $\Delta\phi(\not\!\!E_T, closest - jet)$ in the electron sample.

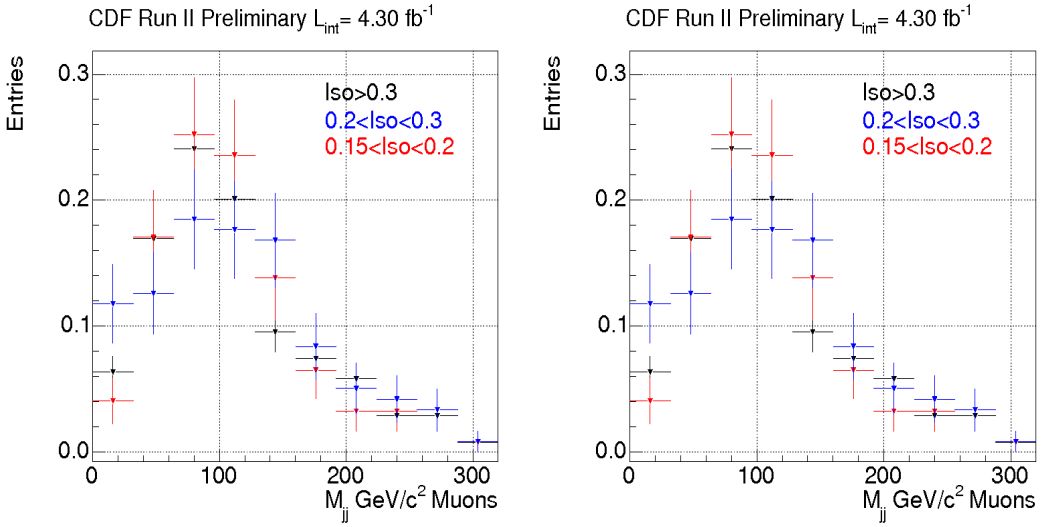

Figure 52: Left: M_{jj} QCD distributions in the muon sample. Right: M_{jj} QCD distributions in the electron sample. Plots are nomalized to unit area.

to the particular QCD selections. We looked at high isolation electrons in place of antielectrons and different isolation selections for muons. We considered events with lepton $0.3 <$ Isolation and $0.15 <$ Isolation < 0.2. Fig.52 shows the standard QCD M_{jj} template overimposed to the alternative ones in the two samples. We do not observe any strange behavior among the templates, but given the low statistics, we will use the alternative templates to asses the systematic uncertainty related to the QCD shape.

13 W+jet: additional Studies

In Sec.11 we compared data and our background expectation in several configurations. We found a good agreement in many kinematic distributions, less agreement was found in the case of ΔR specifially in the electron sample.
To further investigate our W+jet MC using data, we reconstruct Z+2 jets events. A key feature of Z+2 jets sample is that the background is negligible, i.e we can directly compare data and ALPGEN. Unless otherwise indicated, Z+2 jets events are selected by requiring one tight lepton (same selection of w+jet) and one loose lepton with $P_T > 10$ GeV. In addition, the invariant mass M_{ll} of the two leptons is required to be $81 < M_{ll} < 110$ GeV/c^2. Also in this case we require exactly two jets and apply the same selections of w+jet.
Our tests are based on the following assumptions:

- Background in the Z+2 jets sample is negligible. We can directly compare ALPGEN Z+jet Monte Carlo to data.
- If ALPGEN properly models M_{jj} in the Z+jet sample it follows that ALPGEN properly models the W+jet.
- In the case we observe mismodeling in the Z+jet, the same mismodeling affects W+jet and we can extract from Z+jet a correction function $f(M_{jj})$.
- The contribution of the excess in the Z + jet sample is negligible and/or the sample statistics is low enough such that we are not sensitive to the possible resonance.

13.1 Z + jet Data Reweighted to W + jet

In [6], a sample of $\gamma + jet$ events was used to cross check and asses the systematics on the EWK background modeling of the $VV \rightarrow \not\!\!E_T + jj$ analysis. An alternative template for the EWK M_{jj} distribution was extracted from data after applying weights (extracted from MC) to correct for differences between $\gamma + jet$ and EWK.
We use an analogous procedure to extract a M_{jj} template from Z + jet data that is compared to our W + jet MC. We then define, for each M_{jj}^n bin n, the weight $w(M_{jj}^n)$:

$$w(M_{jj}^n) = \frac{MC_{W+jet}(M_{jj}^n)}{MC_{Z+jet}(M_{jj}^n)} \tag{3}$$

that is applied to $Data_{Z+jet}(M_{jj}^n)$. The resulting template is compared to W+jet MC in Fig.53.

We observe a very good agreement between reweighted Z + jet template and W+jet MC both in the muon and electron samples within statistics.
We may use the reweighted Z + jet as and alternative M_{jj} template for our W+jet

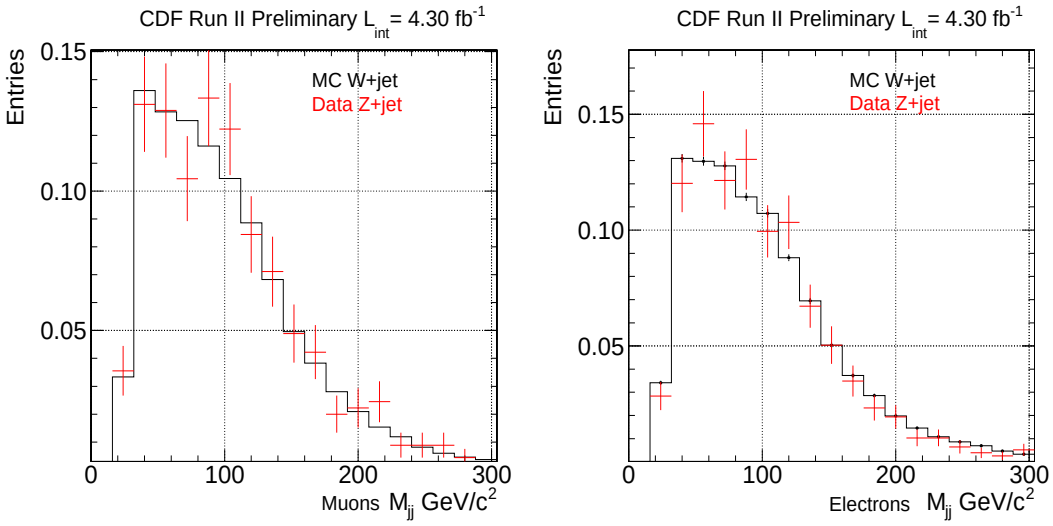

Figure 53: Left: M_{jj} in W+jet MC and Z+jet reweighted data in the muon sample. Right: same for the electron sample. Plots are nomalized to unit area.

systematics, however the statistics is very limited and it would introduce strong fluctuations in our χ^2 fit. We consider this test an additional cross check of ALPGEN M_{jj} modeling in W+jet events.

13.2 Z + jet Data - MC Comparison

We compare the M_{jj} distribution of data Z+jet events to ALPGEN MC. Fig.54 shows the two distributions for muons and electrons respectively. Also in this case, compatible with statistics, we do not observe significant disagreement.

We then look at the ratio of M_{jj} distribution between Z+jet data and ALPGEN MC, Fig.55. If any trend is observed, we can use this ratio to correct W+jet MC. Due to the low statistics, we add together muon and electron samples. We fit the ratio with a first degree polynomial as shown in Fig.55; the fit estimates a small positive slope $(2.79 \pm 4.1) * 10^{-4}$ that is compatible with zero at $\sim 0.7\sigma$ level. Being the slope perfectly compatible with zero, we decide that we do not need to correct our W+jet template. Instead, we use the $\pm 1\sigma$ band functions, red curves in Fig.55, to reweight W+jet. Reweighted templates are considered as alternative shapes used to asses W+jet and Z+jet systematics in our final result.

In Fig.56 we compare the M_{jj} template in W+jet MC to ones after the reweight for $+1\sigma$ and -1σ bands of Fig 55. The same for Z+jet is shown in Fig.57.

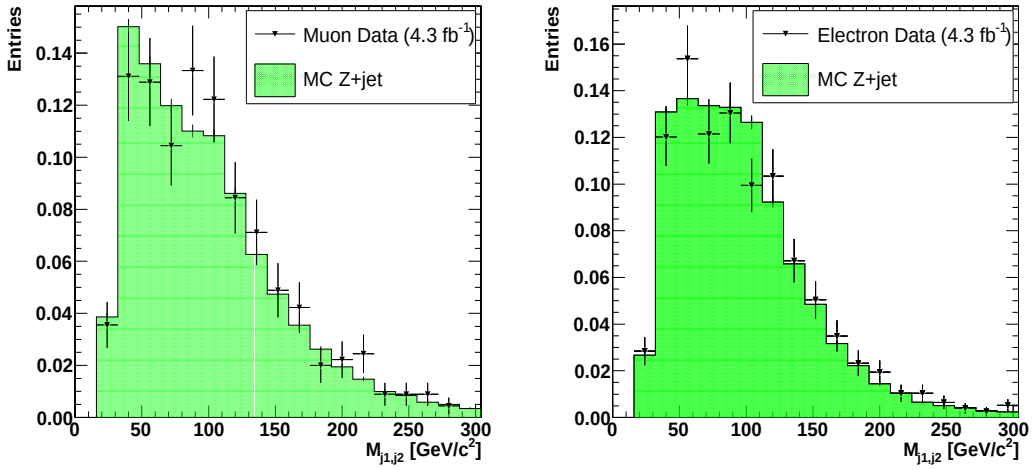

Figure 54: Left: M_{jj} in Z+jet data and MC in the muon sample. Right: same for the electron sample. Plots are nomalized to unit area.

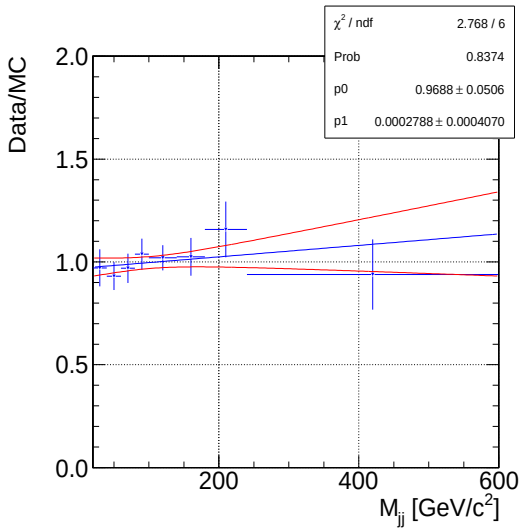

Figure 55: Ratio between Z+jet data and MC M_{jj} distributions adding together muons and electrons; a fit using a first degree polynomial is overimposed and the plus and minus 1 *sigma* line is shown.

14 ΔR Modeling

In Sec.11 we observed disagreement between data and our background model in the ΔR_{jj} distribution, in particular in the electron sample.
The main difference between muons and electrons is the method used to model the

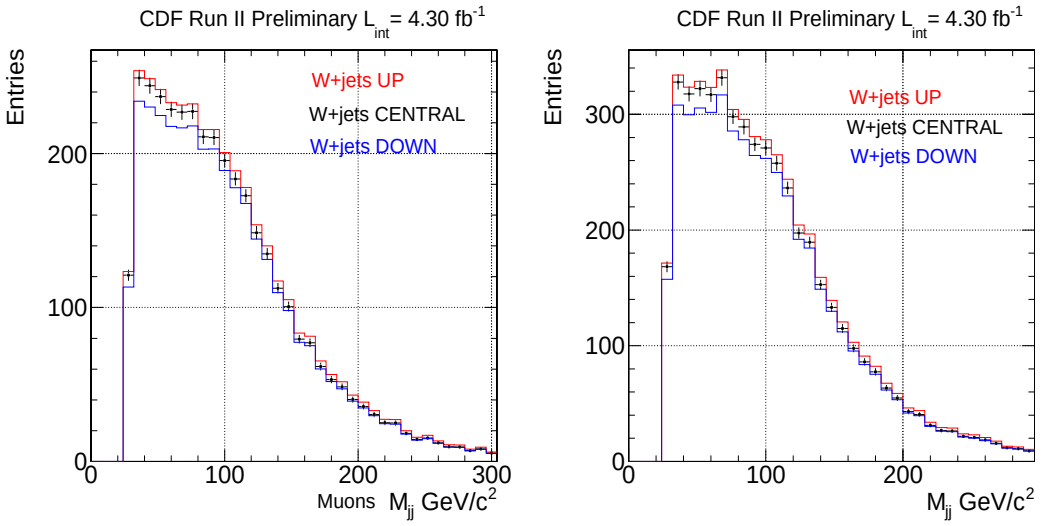

Figure 56: Left: M_{jj} distribution in W+jet MC before (black) and after $+1\sigma$ (red) and -1σ (blue) reweight in the muon sample. Right: same for the electron sample.

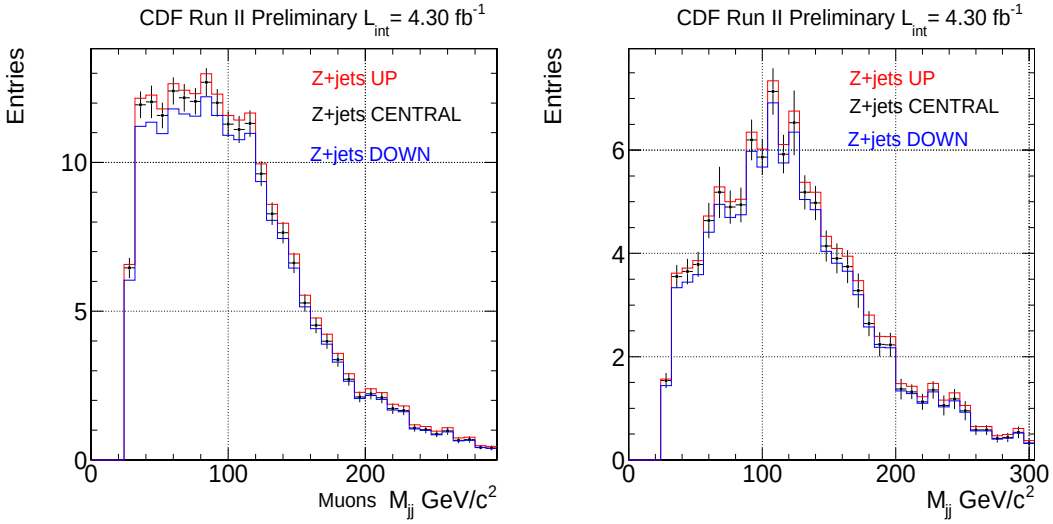

Figure 57: Left: M_{jj} distribution in Z+jet MC before (black) and after $+1\sigma$ (red) and -1σ (blue) reweight in the muon sample. Right: same for the electron sample.

QCD contribution: high isolation candidates for muons and antielectrons for electrons. However, if we compare the ΔR distribution of antieletrons and high isolation electrons, Fig.58, we observe a significant difference and, in particular, high isolation electrons seems to behave such that they may cover the disagreement we see in ΔR. As already discussed in Sec.12, high isolation electrons will be used to asses systematics due to the QCD multijet component.

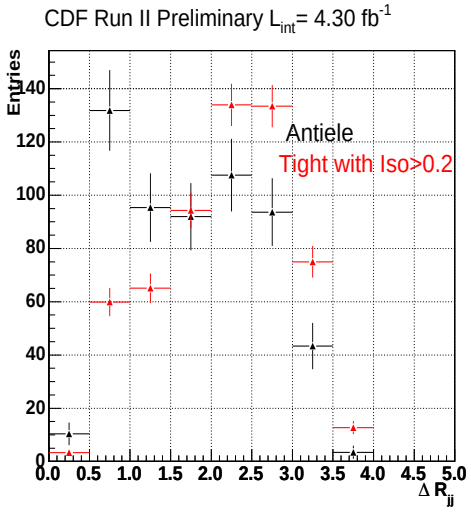

Figure 58: Left: ΔR distribution in antielectron sample (black) and non isolated electrons (red).

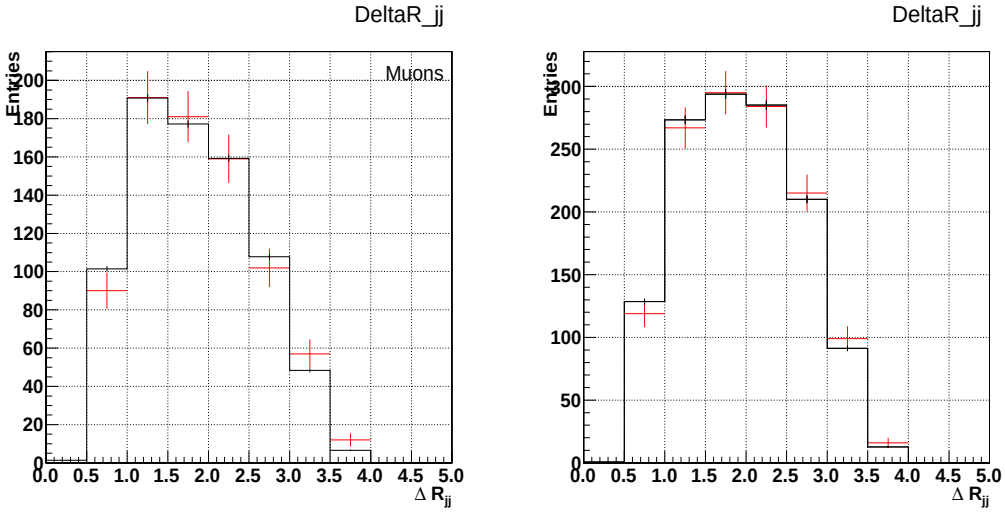

Figure 59: Left: ΔR distribution in Z+jet data and MC in the muon sample. Right: same for the electron sample.

In addition, we can check how the ΔR is modeled in the Z+jet sample. In Fig.59 we compare ΔR in Z+jet data to Z+jet ALPGEN MC. Considering the statistics and given our rather strong selection cuts on jets, we do not observe significant disagreement both in muons and electrons. We then want to check also the effect on ΔR of Z+jet events after applying the M_{jj} reweight obtained in Sec.13.2 and used in W/Z+jet systematics , as we can see in Fig.60.

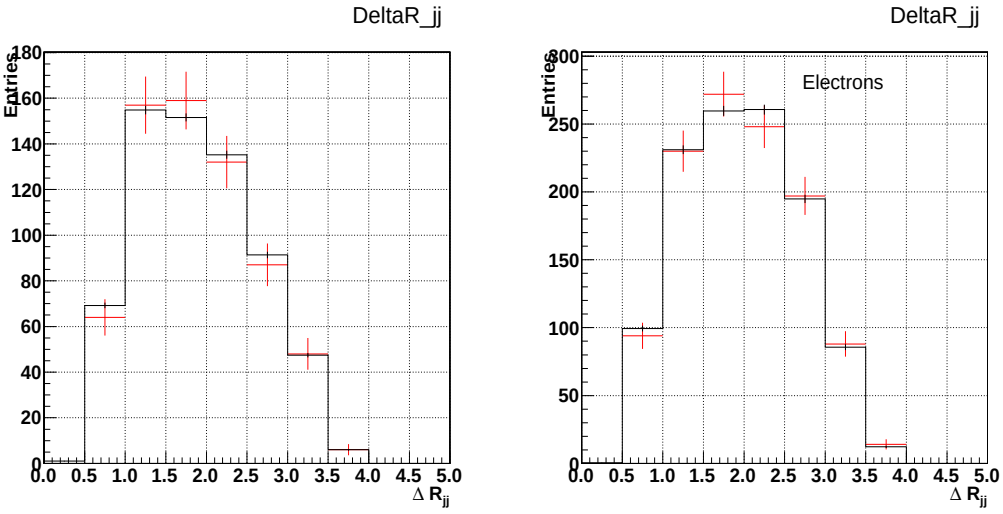

Figure 60: Left: ΔR distribution in Z+jet data and MC after applying $+1\sigma$ band M_{jj} correction in the muon sample. Right: same for the electron sample.

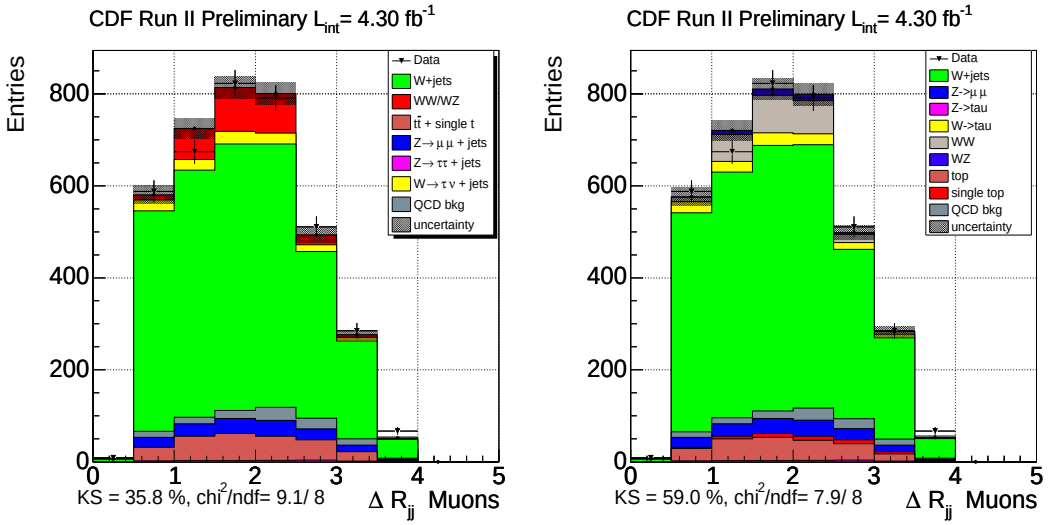

Figure 61: Left: ΔR distribution in data and background expectation before including W/Z+jet systematics in the muon sample. Right: ΔR distribution in data and background expectation including W/Z+jet systematics, again in the muon sample.

Finally, we come back to W+jet sample and look at ΔR in light of what discussed before. As we can observe in Fig.61 and Fig.62, the systematics on the W/Z+jet obtained from the linear fit of previous section and the systematics on the QCD shape cover the ΔR mismodeling.

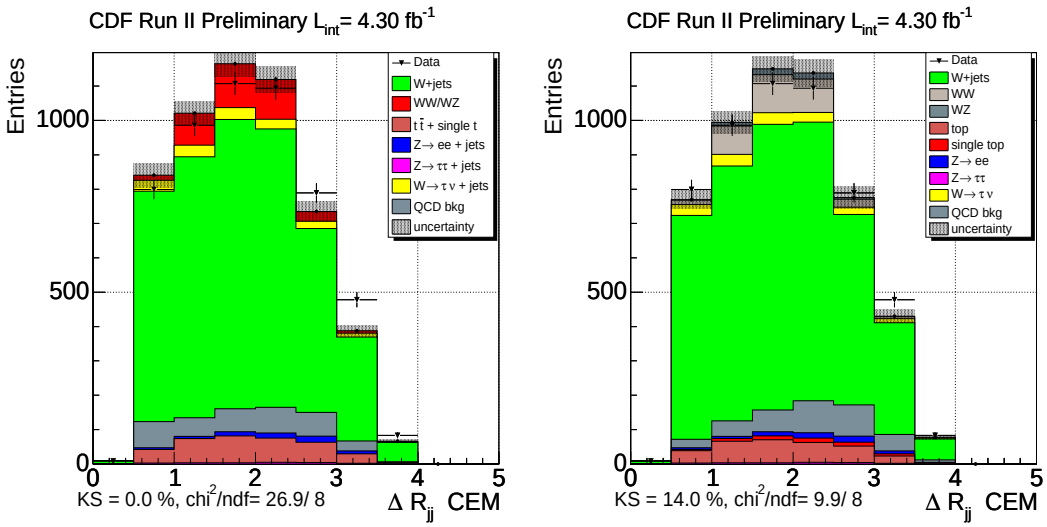

Figure 62: Left: ΔR distribution in data and background expectation before including W/Z+jet systematics in the electron sample. Right: ΔR distribution in data and background expectation including W/Z+jet systematics, again in the electron sample.

15 $t\bar{t}$: Additional Studies

We already studied top enhanced events by requiring three or more jets (section 11). All the kinematical distributions we considered seem to be well modelled. To further test the $t\bar{t}$ MC we consider events with exactly three jets passing selection criteria and we look at the distribution of the invariant mass system of the other combinations of jets, $M_{j1,j3}$ and $M_{j2,j3}$ (63 and 64). A good agreement between data and expectation is observed.

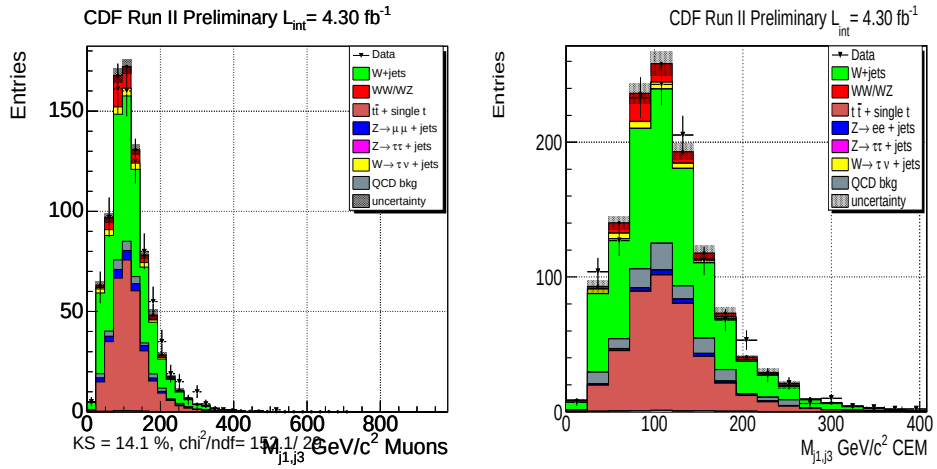

Figure 63: Left: $M_{j1,j3}$ distribution for three jet events in the muon sample. Right: same for the electron sample.

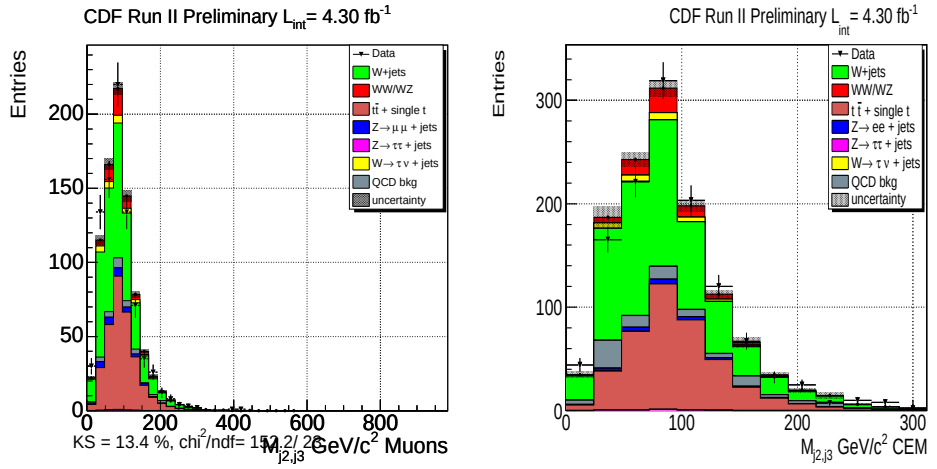

Figure 64: Left: $M_{j2,j3}$ distribution for three jet events in the muon sample. Right: same for the electron sample.

16 Search for a Di-jet Resonance

It would be very difficult to disentangle a di-jet invariant mass peak on top of the W/Z. Because of this, we restrict our search to masses higher than the W/Z M_{jj}. We define our high mass search region to be included in the 120 to 180 GeV M_{jj} interval. In addition, we do not make any assumption on the searched resonance. Since we look for a di-jet resonance the only assumption we make is that the possible signal can be modelled with a gaussian template and its width is compatible with the experimental resolution. We define the expected width to be equal to the $W/Z \to jj$ width scaled to the resonance mass (M) by:

$$\sigma_{resonance} = \sigma_{W/Z}\sqrt{M_{jj}/M_{W/Z}} \tag{4}$$

Using L5 jet corrections we estimate from diboson MC $\sigma_W = 10.5$ and $M_{W/Z} = 77.7$ GeV/c^2.

16.1 Fitting Procedure

The new di-jet resonance, if present, is expected to show up both in the muon and electron samples. Given this contraint, we perform a combined fit of the electron and muon sample for three practical reasons: 1) it should maximize our sensitivity, 2) the unexpected resonance should have the same mass in the two samples, for this reason its mass is constrained to be the same in muons and electrons, 3) the evaluation of the statistical significance is more straightforward.
We perform a χ^2 fit of the M_{jj} spectrum as in the original diboson analysis. We consider 6 components as templates for the fit (both for muons and electrons): W+jets, multijet QCD, Z+jets, $t\bar{t}$ + single top (merged in a single contribution called top), dibosons ($WW + WZ$) and the hypothetical resonance. With the exception of the additional resonance, all the templates are taken from MC or data (for the QCD) and shown in Fig.65 - Fig.69. To avoid strong fluctuations due to the lower statistics with respect to the previous diboson analysis [1], we parameterize the QCD template performing a binned fit as shown in the following sections.
The additional resonance is parameterized as a gaussian distribution whose width is a function of the M_{jj} as defined in eq. (4). The χ^2 is minimized using MINUIT.

The Dibosons, QCD, Z+jets and top are gaussian constrained to their Monte Carlo expectations in the electron and muon sample, respectively. The W+jet contribution is a free parameters in the fit, different for muons and electrons. The hypothetical resonance contribution is a free parameter in the fit , again different for muons and electrons. Moreover, an additive correction α is applied to the diboson template position to take into account possible correction to the Jet Energy Scale (JES). The JES scale factor is gaussian constrained to zero within the JES uncertainty. The fit parameters that are common (constrained to be the same) to the two samples are: the resonance mass and the correction α to the JES enclosed in the diboson template.

The fit is performed in the mass range [28,200] GeV/c^2.

16.1.1 W + jets Template

As W+jets we consider:

- $W \rightarrow l\nu$ + n jets ; $n \geq 0$, $l = e, \mu, \tau$

each single contribution to the M_{jj} shape is extracted by Monte Carlo (see Section 3) and added together in what we consider our template. The relative contribution of each component is determined and fixed by MC. Fig.65 shows the resulting template for the electrons (left) and muons (right).
The total W+jet contribution is a free parameter to be determined by the fit.

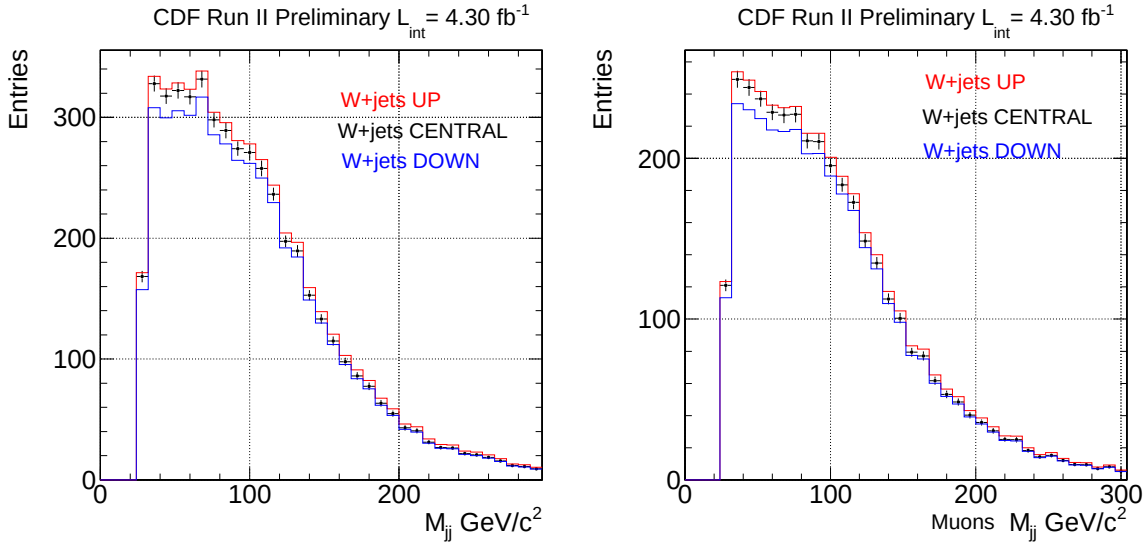

Figure 65: EWK M_{jj} template for electrons (left) and muons (right). Alternative templates obtained from Z+jet data events are superimposed.

16.1.2 QCD Template

In the case of the electron sample, the QCD M_{jj} template is extracted using the anti-electron method; for the muon sample, we select a sample of non isolated muons.
The resulting templates are shown in Fig.66 for electrons (left) and muons (right).

In the M_{jj} fit the QCD component is gaussian-constrained to the value found in the $\not\!\!E_T$ fit with a width of 25%. Since the error on the qcd fraction that comes out of the $\not\!\!E_T$ fit is clearly underestimated, we extract the error on this fraction by performing different fits with different binning and looking at the difference in the measured fraction. The effect of the gaussian constraint on he QCD contribution is negligible.

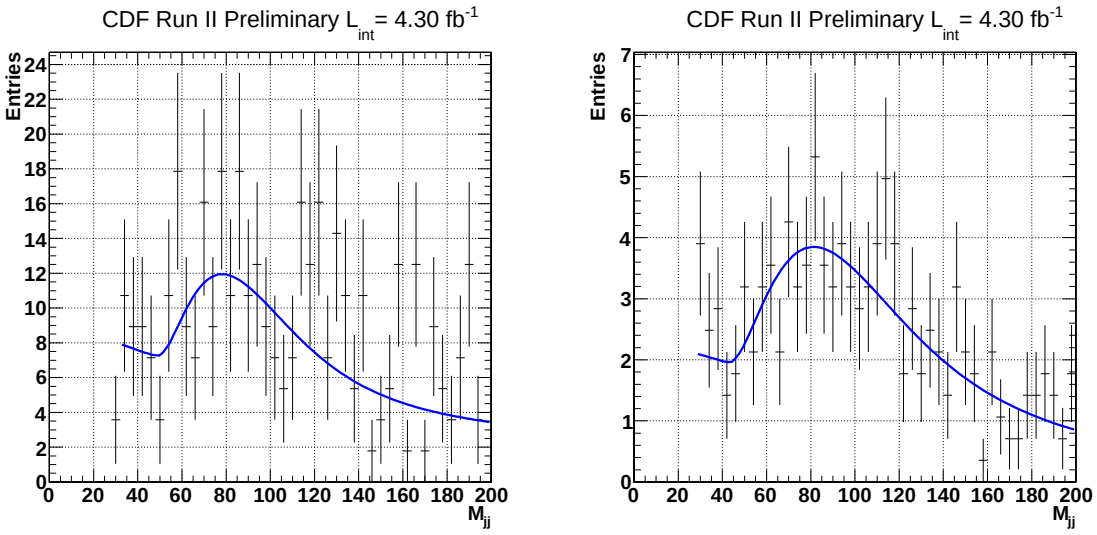

Figure 66: QCD M_{jj} template for electrons (left) and muons (right).

16.1.3 $t\bar{t}$ and Single Top Template

We consider a single template for $t\bar{t}$ and single top (generically called top), added together according to the Monte Carlo expectation. Top normalization is constrained to the theoretical cross section ($t\bar{t}$ + single top) with its error. In Fig.67 we show the corresponding templates for electron and muon samples.

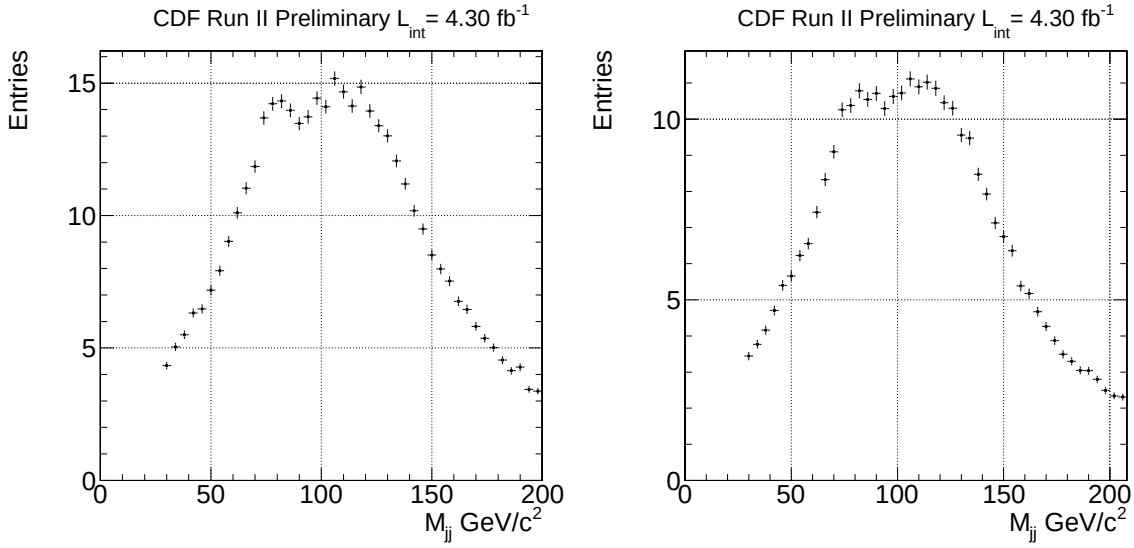

Figure 67: Top ($t\bar{t}$ + single top) M_{jj} template for electrons (left) and muons (right).

16.1.4 Z +jets Template

In Fig.68 we show the corresponding templates for electron and muon samples for the Z+jets background. This background is constrained in the fit to the Monte Carlo expectation.

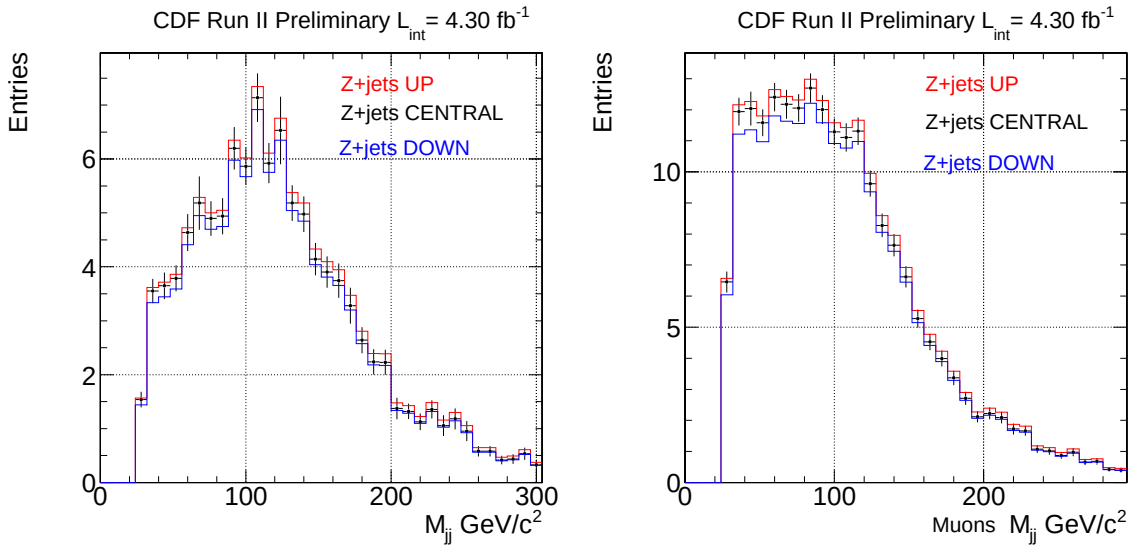

Figure 68: Z+jets M_{jj} template for electrons (left) and muons (right). Alternative templates obtained from Z+jet data events are superimposed.

16.1.5 Diboson Template

The Diboson template, both for electrons and muons channel, are obtained from Monte Carlo combining the WW and WZ, whose relative normalizations are fixed by Monte Carlo.
The resulting templates are shown in Fig.69 for electrons (left) and muons (right). Diboson contribution is gaussian constrained in the main fit to its expectation.

16.2 Fitter validation

We perform some toy studies to validate our fit procedure. Using the previously described templates, 5000 psudoexperiments are generated according to the results of the fit on data, summarized in Tab.9. The residuals, Fig. 70, show that the fit introduces a bias of 2% on the fraction of the additional resonance, completely negligible compared to the statistical error that is of the order of 30% (Tab.9). Moreover the pull distribution shows that the pull width is compatible with one, i.e. MINUIT is properly computing the statistical error.

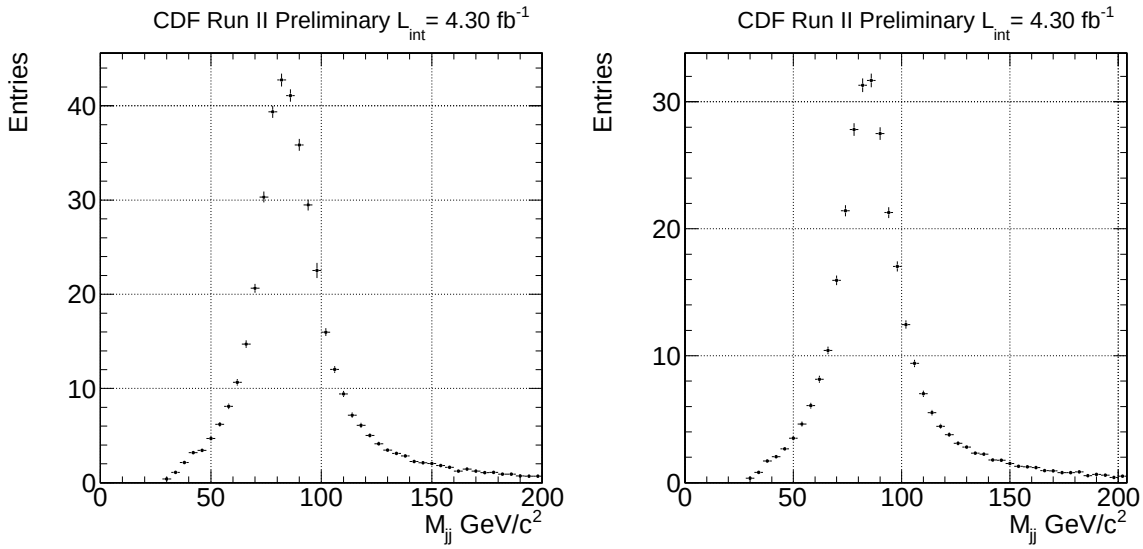

Figure 69: WW/WZ M_{jj} template for electrons (left) and muons (right).

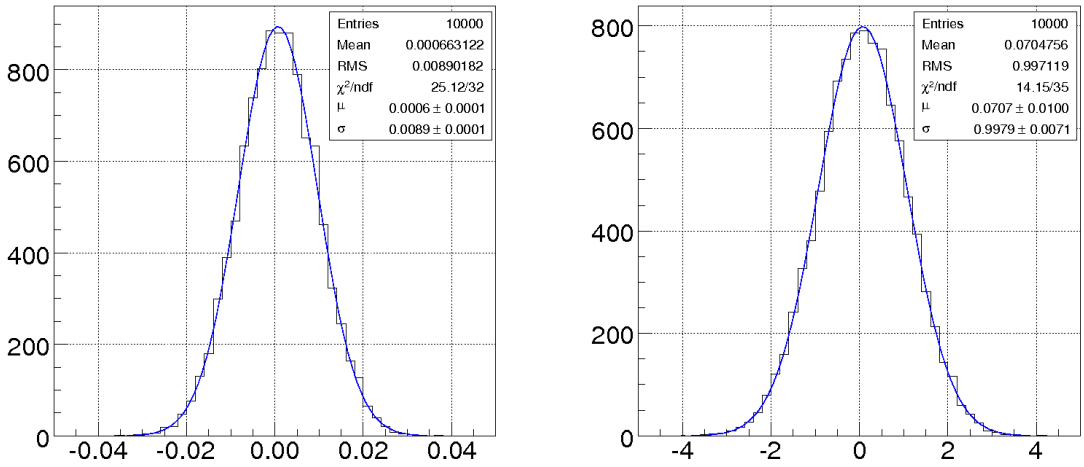

Figure 70: Residual distribution of the additional gaussian component fraction on the left and pull on the right.

17 Dijet Mass Fit

Figure 71 shows the projection of the fit to data using the SM templates only, while in Tab.8 we show the corresponding fit results. We can observe an excess at a mass of about 140 GeV. The χ^2 of the fit still looks reasonable (72.57/84), but the KS test and the run test are poor, 0.00006 and 6 (expected 12 ± 2.3) respectively In what follows, we will refer to this candidate resonance as ACC.

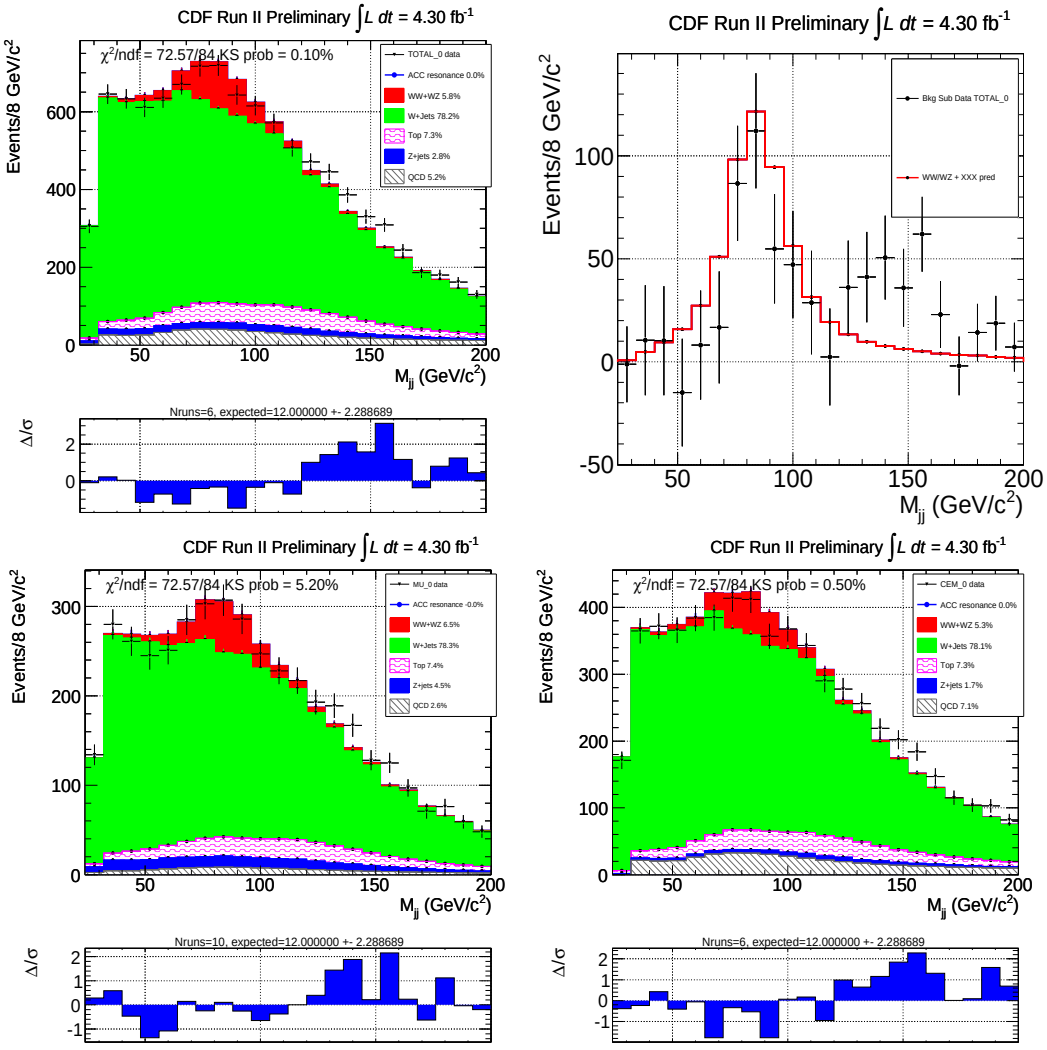

Figure 71: SM fit projections: muons (bottom left), electrons (bottom right), combined (top left) and background subtracted (top right).

Parameter	**Combined**	**CMUP + CMX**	**CEM**
WW + WZ events	–	274.50 ± 37.56	311.97 ± 49.16
WW + WZ exp. events	–	295.13	406.33
σ_{WW+WZ} (pb)	–	14.97 ± 2.05	12.36 ± 1.95
process	fit fraction	exp. fraction	pull
QCD (μ)	0.0260 ± 0.0063	$0.0254 \pm 25.00\%$	0.10
top (μ)	0.0750 ± 0.0071	$0.0727 \pm 10.00\%$	0.31
Z+jets (μ)	0.0452 ± 0.0054	$0.0447 \pm 12.00\%$	0.09
WW+WZ (μ)	0.0658 ± 0.0090	$0.0708 \pm 15.00\%$	-0.47
QCD (ele)	0.0716 ± 0.0154	$0.0654 \pm 25.00\%$	0.38
top (ele)	0.0732 ± 0.0069	$0.0701 \pm 10.00\%$	0.43
Z+jets (ele)	0.0167 ± 0.0020	$0.0164 \pm 12.00\%$	0.15
WW+WZ (ele)	0.0530 ± 0.0084	$0.0691 \pm 15.00\%$	-1.55

Table 8: Fit results without the additional resonance.

Figure 72 shows the standard fit including the additional resonance template for the ACC . In the fit the JES correction is constrained to 0 and WW/WZ is constrained to the standard model cross section, as already mentioned. Considering just the statistical error we estimate significance of 3.64 σ. In the main fit, the ACC width is fixed to the one we expect from the experimental resolution (14.7 GeV). If we leave the width free in the fit, we estimate a width of 15.6 ± 6.5 GeV, compatible with the expectation, while the ACC significance (without considering systematics) is 3.4σ. It is also worth noticing that the region around 40-60 GeV that does not fit well in figure 71 is now properly described by the fit with the addition of the gaussian component. This indicates that the SM templates cannot fit the data in the region 40-60 and 130-160 GeV, unless we assume the existence of an additional, resonance like, contribution. Indeed the χ^2 improves by 20.45 and both the KS and run tests are very satisfactory: 0.756 and 11 (expected 12 ± 2.3) respectively.
In Tab.9 we show the fit results including the extra resonance. We estimate 255 ± 58 ACC events in our electron plus muon samples (statistics only). The gaussian mean value is estimated to be 144.46 ± 4.69.
If we leave the Diboson JES correction α free to float in the fit, we estiamate $\alpha = 0.007 \pm 0.03$ and the ACC significance is 3.64 σ.

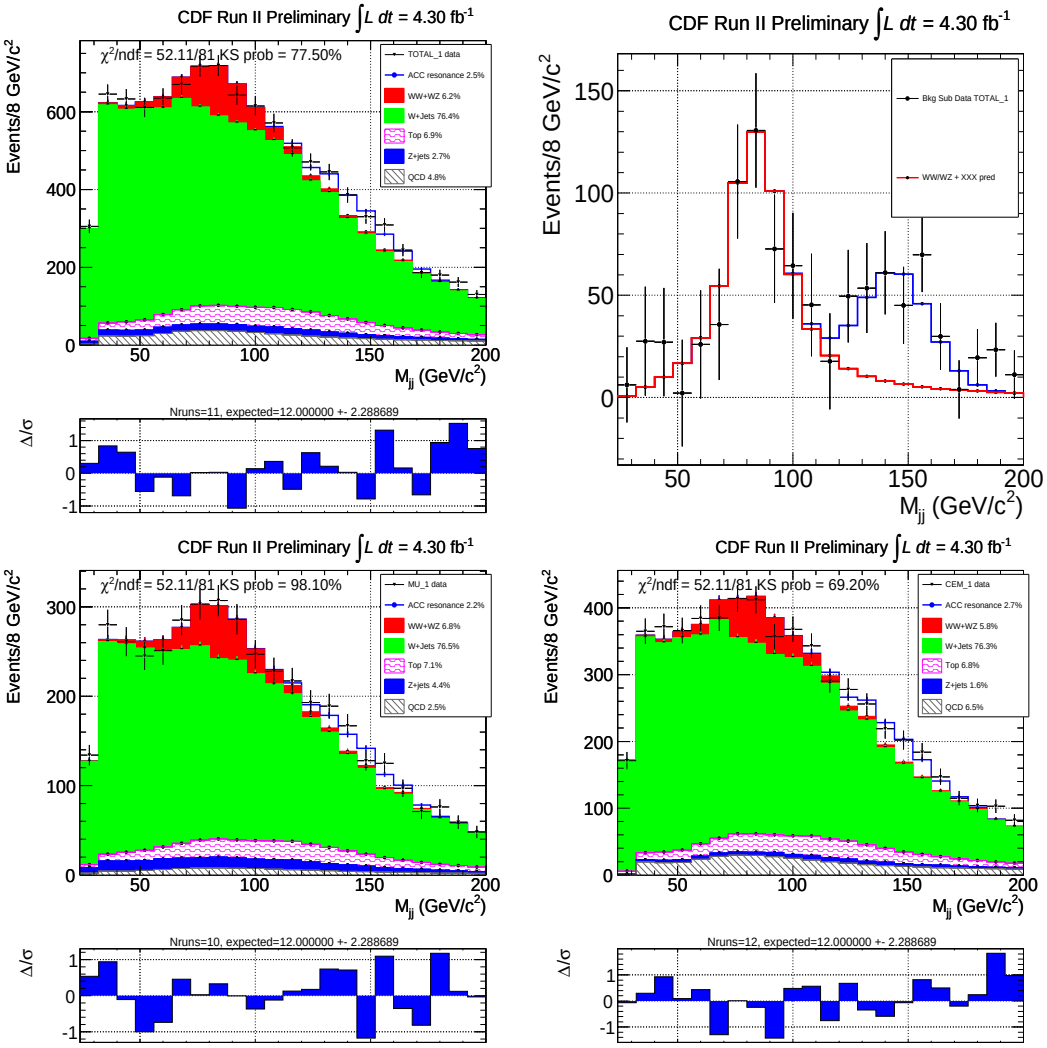

Figure 72: Fit projections with SM backgrounds and a gaussian template for the excess: muons (bottom left), electrons (bottom right), combined (top left) and background subtracted (top right).

Parameter	**Combined**	**CMUP + CMX**	**CEM**
WW + WZ events	–	285.43 ± 37.63	341.16 ± 48.81
WW + WZ exp. events	–	288.95	395.77
σ_{WW+WZ} (pb)	–	15.90 ± 2.10	13.88 ± 1.99
process	fit fraction	exp. fraction	pull
QCD (μ)	0.0254 ± 0.0063	$0.0254 \pm 25.00\%$	0.01
top (μ)	0.0729 ± 0.0072	$0.0727 \pm 25.00\%$	0.01
Z+jets (μ)	0.0449 ± 0.0054	$0.0447 \pm 12.00\%$	0.03
WW+WZ (μ)	0.0699 ± 0.0092	$0.0708 \pm 15.00\%$	-0.08
QCD (ele)	0.0667 ± 0.0153	$0.0654 \pm 25.00\%$	0.08
top (ele)	0.0701 ± 0.0069	$0.0701 \pm 25.00\%$	-0.00
Z+jets (ele)	0.0164 ± 0.0020	$0.0164 \pm 12.00\%$	0.03
WW+WZ (ele)	0.0595 ± 0.0085	$0.0691 \pm 15.00\%$	-0.92
ACC events	–	92.79 ± 37.83	161.94 ± 44.08
$\sigma_{ACC}^{WWacceptance}$ (pb)	–	5.17 ± 2.11	6.59 ± 1.79
ACC mass (GeV/c^2)	144.46 ± 4.69	–	–
ACC width (GeV/c^2)	14.70 ± 0.00	–	–
	χ^2 **NH**	χ^2 **RH**	$\Delta\chi^2$
Goodness of Fit	72.57	52.11	20.45
	p-value	significance (σ)	
	1.37e-04	3.64	–

Table 9: Fit results for $M_{jj} \in [28,200]$ GeV/c^2 including the extra resonance ACC. In the lower row there are the fit χ^2 without the extra resonance (NH), fit χ^2 with the extra resonance (RH) and the corresponding $\Delta\chi^2$.

18 Systematics: data driven procedure

We asses the systematic uncertainty on the ACC extraction considering different sources. These systematics will affect the number of ACC events we estimate in our data sample and the corresponding significance.
On the other hand, since we do not focus on any specific model for the additional resonance search we cannot estimate the acceptance of the ACC and quote the corresponding cross section. As a consequence, we will consider only the systematics affecting the signal extraction.
If not otherwise stated, we estimate the systematics on by generating pseudo-experiment using an alternative template model for each systematic source. The pseudo-experiments are then fitted using the templates used in the main fit.
The difference between the central value of the fit on data and the mean of the estimator of the signal content on the alternative pseudo-experiment is taken as systematics on the corresponding source.
In general, Jet Energy scale does not affect the QCD template since it is extracted from an independent data sample; similarly, also ALPGEN W+jet and Z+jet (with one lost leg) templates are corrected by looking at an independent data sample. In addition, as shown in Section 17, when the diboson JES correction is free in the fit, we find a value compatible with one and the fit result is not affected at all by the additional parameter. Finally, the ACC template mean value is completely free in the fit. As a consequence, we do not asses systematics due to the JES with the exception of the top contribution, as discussed in next sections.
We consider systematics associated with the W+jet and Z+jet, the QCD tamplate shape and JES effect on top template. In Tab.10 we summarize each systematics contribution; values are expressed as % on the ACC number of events. In the following sections we describe how the systematics associated to each source has been evaluated.

	Source	**%**
Signal Extraction	ALPGEN reweight up	-4.5%
	ALPGEN reweight down	+6.2%
	QCD up	-6.2%
	QCD down	-6.2%
	JES up ($t\bar{t}$ and single top)	+6.3%
	JES down ($t\bar{t}$ and single top)	-6.3%
TOTAL		10.3 %

Table 10: Systematics uncertainties: effect, in percentage, on the number of ACC events.

18.1 ALPGEN MC

We already discussed the procedure used to extract alternative W/Z + jet templates to asses the corresponding systematics in Sec. 13.2. A good property of this procedure is that it incorporates any M_{jj} mismodeling of ALPGEN MC and, since it is extracted from data, we do not need to add contributions, for example, due to the generation Q^2 or uncertainties on the Jet Energy Scale.
The two systematics functions used to reweight W/Z + jet MC are shown in Fig.73 and corresponds to the $\pm 1\sigma$ band of the first order polynomial fit. Fig.74 and Fig.74 show the W+jet and Z+jet templates reweighted for systematics, both for muons and electrons.

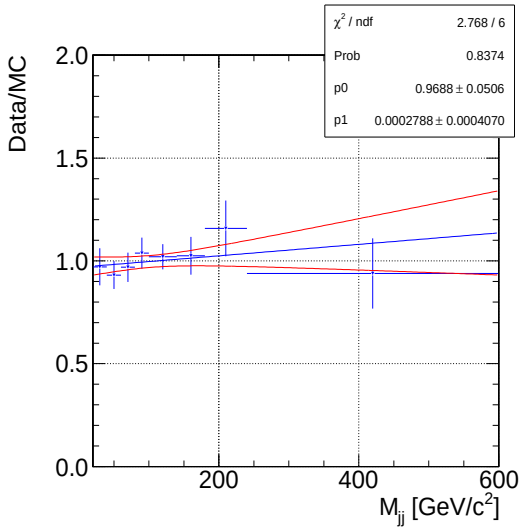

Figure 73: Fit of the ratio between Z+jet M_{jj} in data and ALPGEN MC using a first order polynomial.

18.2 QCD

As mentioned in Section 12, to evaluate the systematic associated with the QCD shape, we look at non-isolated electrons in place of antielectrons and different isolation selections for muons. We considered events with lepton Isolation > 0.3 and $0.2 >$Isolation > 0.15. The resulting M_{jj} templates are used as systematics. Fig.76 shows the standard QCD M_{jj} template overimposed to the alternative ones in the two samples. In our main fit, QCD fraction is constrained to what we estimated in the $\not\!\!E_T$ fit; leaving QCD completely free in the central fit does not affect the ACC contribution. For this reason we do not assign any systematics due to the QCD normalization.

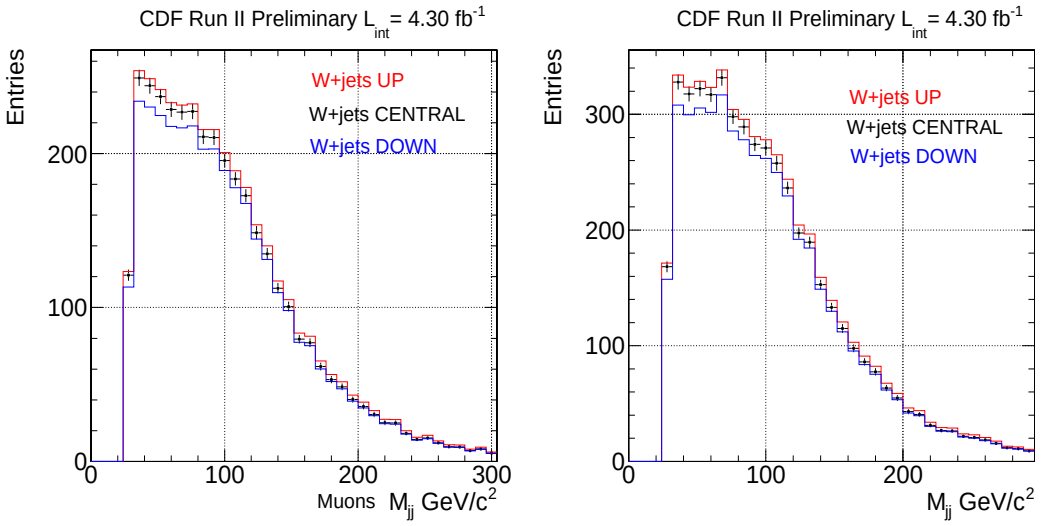

Figure 74: W+jet used in systematics evaluation overimposed to the main fit tempaltes for muons (left) and electrons (right).

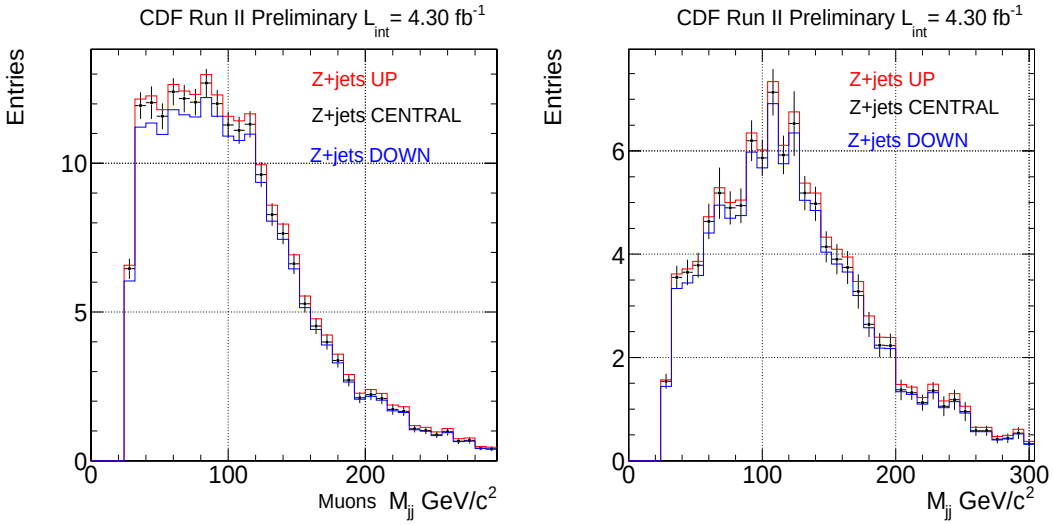

Figure 75: Z+jet used in systematics evaluation overimposed to the main fit tempaltes for muons (left) and electrons (right).

18.3 $t\bar{t}$ + Single Top

Jet Energy Scale uncertainties may affect only the top contribution. We then extract alternative templates for $t\bar{t}$ + Single Top by varying the Jet Energy Scale of $\pm 1\sigma$ with respect to the nominal value. Fig.77 shows the standard $t\bar{t}$ + Single Top M_{jj} template overimposed to the alternative ones in the muon and electron samples.

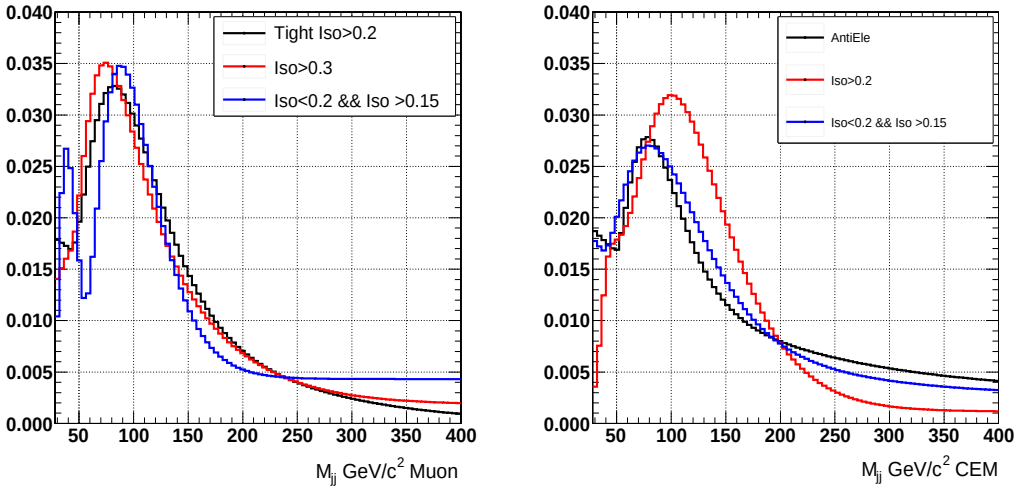

Figure 76: Left: QCD M_{jj} alternatve templates in the muon sample. Right: QCD M_{jj} alternative templates in the electron sample.

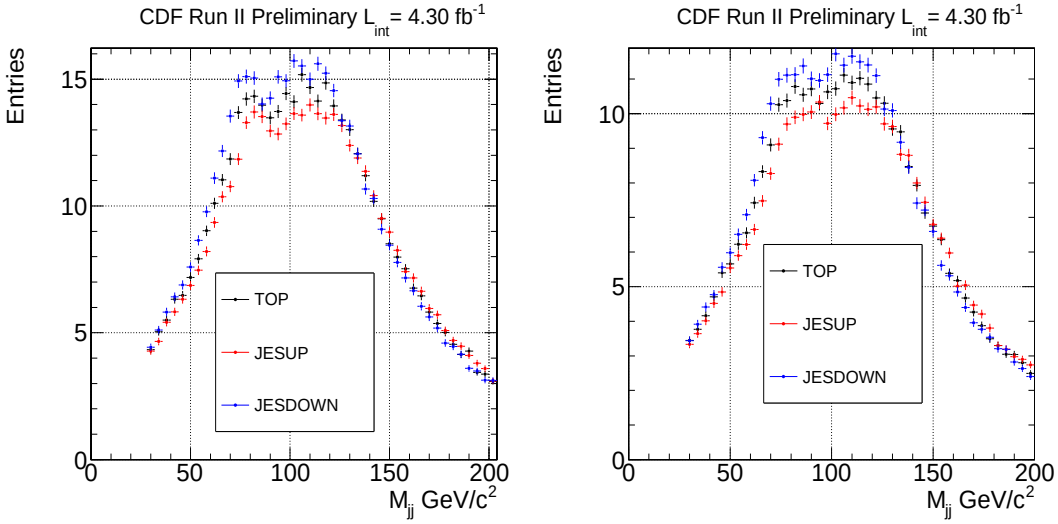

Figure 77: Left: $t\bar{t}$ + Single Top M_{jj} alternative templates in the muon sample. Right: M_{jj} $t\bar{t}$ + Single Top M_{jj} alternative templates in the electron sample.

19 Systematics: standard procedure

Up to this point we have talked about an essentially data driven strategy to asses systematics uncertainty. Instead, we are also interested in looking at a different approach and asses systematics by considering standard (at CDF) effects: Jet Energy Scale up and down ($\pm 1\sigma$ of the corresponding value) on all MC templates, ALPGEN Q^2 up and

down using alternative W/Z+jet MC samples, and the same QCD alternative templates shown before.
We will use the standard procedure to quote the results of this analysis, while the data driven approach, very conservative and limited by the $Z + jet$ data sample statistics, will be considered an interesting crosse check of the analysis. In particular, the $Z + jet$ procedure attempts to test on data whether the observed excess might be due to a less than perfect modeling of $W + jets$ by the Monte Carlo or to the presence of additional physical process.
In Tab.11 we show the effect on the number of estimated ACC events. In the following sections, after discussing the procedure we use to evaluate the significance of the ACC including systematics effects, we will also quote the corresponding significance.

	Source	e %	μ %
Signal Extraction	Q^2 up (W/Z+jet)	-4.5%	-3.9 %
	Q^2 down (W/Z+jet)	+6.2%	+6.1%
	QCD up	-6.2%	-6.1%
	QCD down	-6.2%	-6.1%
	JES up (all, except QCD)	+6.3%	+5.1%
	JES down (all, except QCD)	-6.3%	-5.1%
TOTAL		10.3 %	9.0 %

Table 11: Systematics uncertainties: effect, in percentage, on the number of ACC events.

20 P-Value

To evaluate the significance of the resonance, we apply the same procedure of [1]. Suppose we have a given number N_{syst} of systematics sources , we generate a toy MC sample for each combination of the N_{syst}, i.e. in each sample, some of the systematics are varied. For each sample, we evaluate the corresponding p-value using the $\Delta\chi^2$ between the background only and signal hypothesis as test statistics. The significance we quote for our result is the worst among the p-values we obtain. For each systematics combination, we generate and fit 1 million samples. To take into account the trial factor, in our toy experiments we scan the mass of the resonance in the search region [120 - 180] GeV/c^2 using steps of 4 GeV/c^2 and evaluate, at each step, the corresponding χ^2: for each toy sample, the minimum χ^2 of the scan is used in the $\Delta\chi^2$ evaluation.
If we consider as our systematics sources the ones described in Sec.19, the worst p-value comes from Q^2 Up, JES up and QCD up scenario and returns a p-value of 7.1* 10^{-4} that corresponds to a significance of approximatively 3.2 σ. The corresponding $\Delta\chi^2$ distribution is shown in Fig.78.

If we check this result with a more conservative approach using the data driven

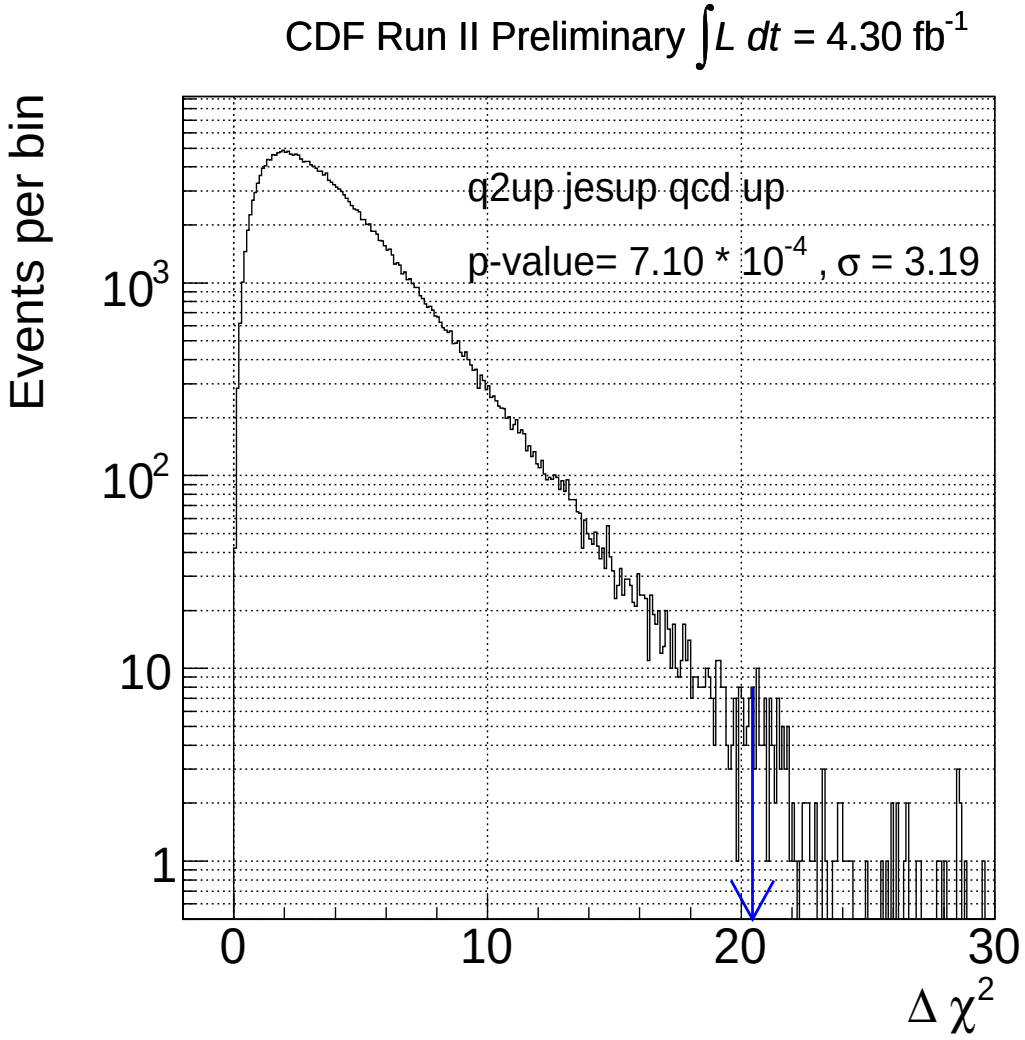

Figure 78: $\Delta\chi^2$ distribution of the Q2 Up, JES up and qcd up scenario.

systematics discussed in Sec.18, the worst p-value comes from the W/Z+jet up and QCD up scenario and returns a p-value of 0.0010 that corresponds to a significance of approximatively 3.09 σ.

21 Scan in Jets E_T and comparison with Higgs MC

We apply different jet E_T cuts to verify that the resonance is still in place using other selections. In particular, we fit the M_{jj} spectrum including the extra resonance term for several jet E_T selections.
For simplicity, these χ^2 fits are performed using histograms for QCD templates and they are not smoothed using an analytical function. As shown in Fig.79 - Fig.81 the

ACC contribution is not negligible in all cases . As expected for a physical process, by increasing the jet E_T threshold, the signal does not disappear. In Table 12 are shown the fit results for Higgs compared to ACC production.
We also compare the behavior of the ACC with a MC sample of WH with $M_H = 150$ GeV/c^2. As we can see in table 12 the ACC mean value increases as expected by the Higgs MC. Furthermore, we show that the efficiency of ACC and Higgs, normalized to the number of events estimated at $E_T > 30$ GeV, are in very good agreement. These numbers are extracted from the fit for the ACC and calculated from MC for the Higgs (this comparison is fair in the hypothesis of unbiassed fit, as shown in previous sections).

jet E_T	**H Mass (MC)**	**ACC Mass (fit)**	**ACC # eve**	ϵ_{ACC}	ϵ_{Higgs}
$E_T > 30$	130.1	149.0 ± 4.8	211		
$E_T > 35$	131.7	150.4 ± 4.8	192	0.91	0.83
$E_T > 40$	132.6	153.3 ± 4.1	159	0.73	0.67
$E_T > 45$	134.2	156.7 ± 4.7	119	0.56	0.53
$E_T > 50$	136.5	156.8 ± 5.7	102	0.48	0.41
$E_T > 55$	137.7	162.4 ± 6.1	62	0.29	0.31
$E_T > 60$	138.4	162.8 ± 6.2	36	0.17	0.23
$E_T > 65$	139.2	164.0 ± 7.3	22	0.10	0.15

Table 12: Fit results for $M_{jj} \in$ [28,200] GeV/c^2 applying different jet E_T cuts.

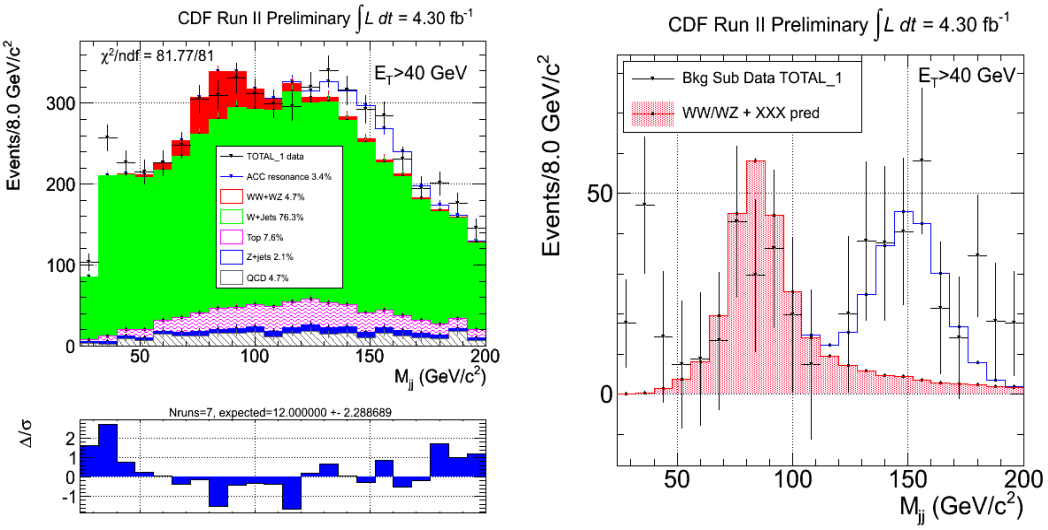

Figure 79: Left: Fit to the M_{jj} shape for events that have two jets with $E_T > 40$ GeV . Right: Background subtracted data with MC prediction

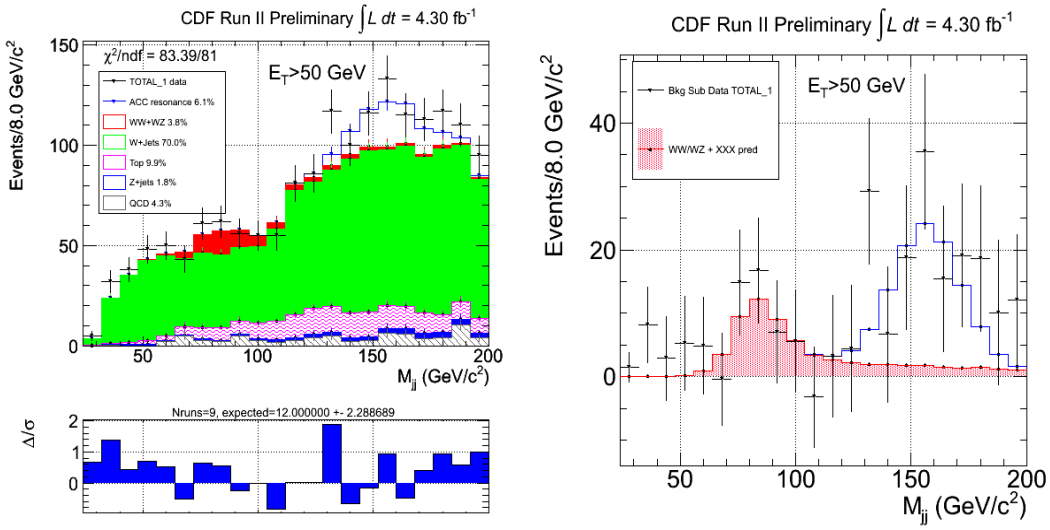

Figure 80: Left: Fit to the M_{jj} shape for events that have two jets with $E_T > 50$ GeV . Right: Background subtracted data with MC prediction

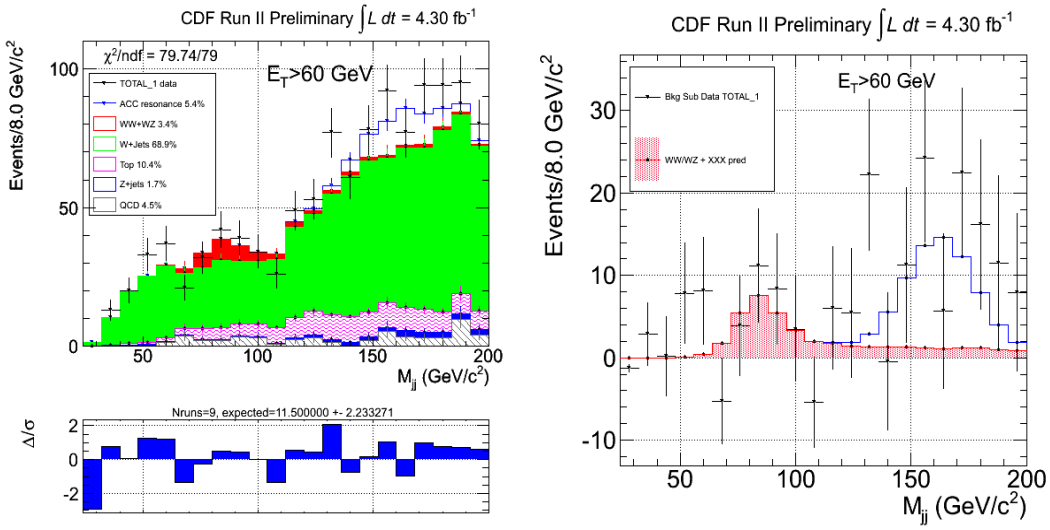

Figure 81: Left: Fit to the M_{jj} shape for events that have two jets with $E_T > 60$ GeV . Right: Background subtracted data with MC prediction

22 Wider Mass Range Fit

Fig. 82 shows the fit extened up to 300 GeV. The results of the fit are shown in Table 13. The significance decreases because of the trial factor since we are considering a wider search window. The yellow band in the background subtracted plot represents data driven systematic uncertainties.

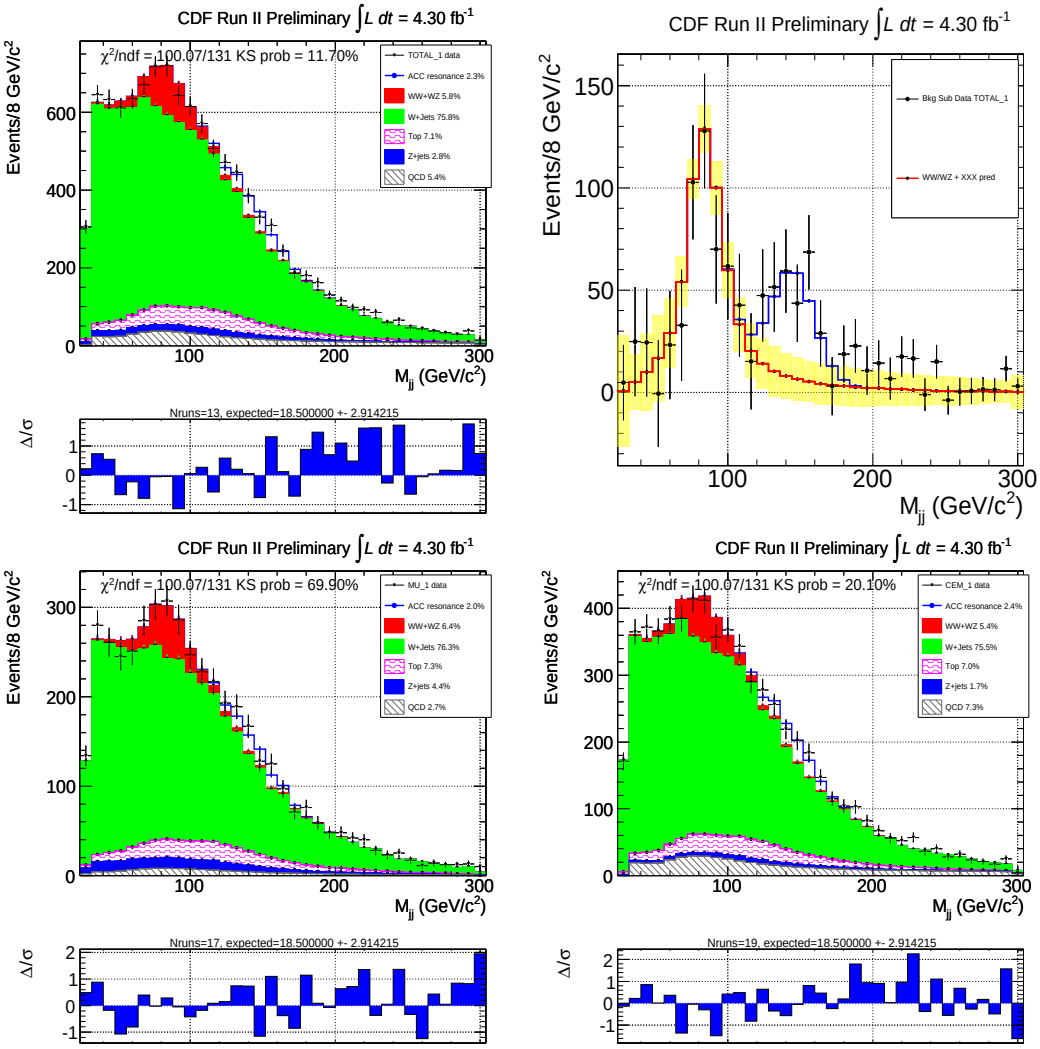

Figure 82: Fit of data in the range 28-296 GeV with SM backgrounds and a gaussian for the excess at m_{jj} about 150 GeV: : muons (bottom left), electrons (bottom right), combined (top left) and background subtracted (top right).

Parameter	**Combined**	**CMUP + CMX**	**CEM**
WW + WZ events	–	288.30 ± 37.92	345.63 ± 48.81
WW + WZ exp. events	–	295.77	406.86
σ_{WW+WZ} (pb)	–	15.69 ± 2.06	13.68 ± 1.93
process	fit fraction	exp. fraction	pull
QCD (μ)	0.0274 ± 0.0066	$0.0269 \pm 25.00\%$	0.07
top (μ)	0.0750 ± 0.0073	$0.0745 \pm 25.00\%$	0.03
Z+jets (μ)	0.0453 ± 0.0054	$0.0451 \pm 12.00\%$	0.03
WW+WZ (μ)	0.0660 ± 0.0087	$0.0678 \pm 15.00\%$	-0.17
QCD (ele)	0.0735 ± 0.0130	$0.0701 \pm 25.00\%$	0.20
top (ele)	0.0722 ± 0.0070	$0.0717 \pm 25.00\%$	0.03
Z+jets (ele)	0.0172 ± 0.0021	$0.0171 \pm 12.00\%$	0.06
WW+WZ (ele)	0.0560 ± 0.0079	$0.0659 \pm 15.00\%$	-1.00
ACC events	–	88.23 ± 37.20	156.90 ± 36.35
$\sigma_{ACC}^{WWacceptance}$ (pb)	–	4.80 ± 2.02	6.21 ± 1.44
ACC mass (GeV/c^2)	144.71 ± 4.53	–	–
ACC width (GeV/c^2)	14.70 ± 0.00	–	–
	χ^2 **NH**	χ^2 **RH**	$\Delta\chi^2$
Goodness of Fit	120.29	100.74	19.55
	p-value	significance (σ)	
	2.10e-04	3.53	–

Table 13: Fit result for fit with a wider mass range

23 Conclusions

We report a study of composition and shape of the invariant mass spectrum of jet pairs produced in association with a W boson decaying into leptons (electrons and muons). The measured mass spectrum is interpreted as the superposition of known backgrounds ($t\bar{t}$, single top, Z+jets, QCD multijets), di-boson production (WW, WZ), and W+jets. The shapes of the background components are obtained from Monte Carlo plus full CDF detector simulation except for QCD multijet where the shape is obtained from data.
The best fit of the known components shows a good agreement with the data except for the [120, 160] mass range where an excess is observed in both electron and muon data, suggestive of a possible resonance structure.
To assess the significance of the excess we perform a standard $\Delta\chi^2$ test of the hypothesis of the presence of a gaussian bump in addition to all known components. The width of the gaussian is fixed to the expected two jet mass resolution for a given value of the mass and the mean is unknown.
The test returns a p-value of $7.4 * 10^{-4}$ corresponding to a significance of 3.2 σ when standard systematics sources are considered.
If we test this result using $Z + jet$ data events, we obtain a p-value of 0.0010 that corresponds to approximatively 3.09 σ. This test does not reject the hypothesis of an additional physical process.

References

[1] Annovi, Catastini, Cavaliere, Ciocci, Duchini, Mastrandrea, Rescigno CDF Note 10003.

[2] Annovi, Catastini, Cavaliere, Ciocci, Mastrandrea, Rescigno, Sfyrla CDF Note 9807.

[3] T.Spreitzer *et al.*,"Electron Identification in Offline Release 6.1.2", CDF Note 7950.

[4] J. Adelman *et al.*, Method II For You, CDF Note 9185.

[5] B. Cooper, A. Messina, "Estimation of the Background to W e + n Jet Events", CDF note no. 6636.

[6] G. Flanagan, J Freeman, S. Pronko, V. Rusu, CDF Note 9736.

[7] CDF/ANAL/BOTTOM/PUBLIC/9458.